SCIENCE IMMUNOLOGY | RESEARCH ARTICLE

MACROPHAGES

SLAMF7 engagement superactivates macrophages in acute and chronic inflammation

Daimon P. Simmons[1,2], Hung N. Nguyen[2,3], Emma Gomez-Rivas[3], Yunju Jeong[2,4], A. Helena Jonsson[2,3], Antonia F. Chen[2,5], Jeffrey K. Lange[2,5], George S. Dyer[2,5], Philip Blazar[2,5], Brandon E. Earp[2,5], Jonathan S. Coblyn[2,3], Elena M. Massarotti[2,3], Jeffrey A. Sparks[2,3], Derrick J. Todd[2,3], Accelerating Medicines Partnership (AMP) RA/SLE Network†, Deepak A. Rao[2,3], Edy Y. Kim[2,4], Michael B. Brenner[2,3]*

Macrophages regulate protective immune responses to infectious microbes, but aberrant macrophage activation frequently drives pathological inflammation. To identify regulators of vigorous macrophage activation, we analyzed RNA-seq data from synovial macrophages and identified SLAMF7 as a receptor associated with a superactivated macrophage state in rheumatoid arthritis. We implicated IFN-γ as a key regulator of SLAMF7 expression and engaging SLAMF7 drove a strong wave of inflammatory cytokine expression. Induction of TNF-α after SLAMF7 engagement amplified inflammation through an autocrine signaling loop. We observed SLAMF7-induced gene programs not only in macrophages from rheumatoid arthritis patients but also in gut macrophages from patients with active Crohn's disease and in lung macrophages from patients with severe COVID-19. This suggests a central role for SLAMF7 in macrophage superactivation with broad implications in human disease pathology.

INTRODUCTION

Macrophages are necessary for protection against infectious microbes (*1*) but can drive acute inflammation that can become exuberant or chronic and cause profound tissue pathology (*2*). Dysfunctional macrophage activation is evident in autoimmune diseases including rheumatoid arthritis (RA) (*3*–*5*), inflammatory bowel disease (IBD) (*6*–*8*), and interstitial lung disease (*9*, *10*). RA is characterized by infiltration of macrophages into the synovium, along with populations of lymphocytes and activated stromal cells (*11*–*15*). Macrophage numbers and activation states change and can correlate with response to therapy in RA (*16*–*18*). In respiratory infection, macrophages promote inflammation resulting in lung injury (*19*) and contribute to immune activation in severe acute respiratory disease syndrome (*20*, *21*) associated with coronavirus disease 2019 (COVID-19) (*22*, *23*).

Macrophage activation states are determined by receptors for an array of environmental signals (*24*), with cytokines and microbial molecules as the best-known macrophage regulators (*25*–*27*). Interferon-γ (IFN-γ) is a key component of classical "M1" macrophage activation (*27*) and potentiates macrophage responses to subsequent stimulation (*28*–*30*). Toll-like receptor (TLR) agonists prime macrophages to express inflammasome components that, when activated, result in pyroptotic cell death and release of bioactive interleukin-1β (IL-1β) (*31*).

Here, we find that an important component of the macrophage response to a primary signal is up-regulation of a secondary superactivator receptor that can then transform these primed or potentiated macrophages into a highly activated, potentially pathogenic inflammatory state. As a strategy to find key regulators of superactivated macrophages (SAMs), we evaluated inflammatory human diseases where macrophages are implicated as major drivers of inflammation. Using this approach, we identified signaling lymphocytic activation molecule family member 7 [SLAMF7, also known as CD319, CD2-like receptor-activating cytotoxic cell (CRACC), and CS1] (*32*–*34*) and implicate this receptor as having a central role in highly activated macrophage-related inflammatory diseases. We determined that SLAMF7 is selectively expressed by macrophages from sites of inflammation and is regulated by IFN-γ. Engagement of the receptor drove a strong inflammatory signature, activating nuclear factor κB (NF-κB) and mitogen-activated protein kinase (MAPK) pathways, along with further autocrine amplification by tumor necrosis factor–α (TNF-α). In publicly available single-cell RNA sequencing (RNA-seq) data, we found this SLAMF7-SAM population in diverse tissues not only from patients with RA but also from patients with IBD and COVID-19 pneumonia. This implicates SLAMF7 activation of inflammatory macrophages as a key pathway driving pathology in acute and chronic inflammatory human diseases.

RESULTS

Up-regulation of SLAMF7 on macrophages from inflamed synovial tissue

We focused on the inflammatory human disease RA to identify signaling receptors that could act as macrophage superactivators. We analyzed publicly available bulk RNA-seq data from phase 1 of the Accelerating Medicines Partnership (AMP) Rheumatoid Arthritis/Systemic Lupus Erythematosus Network (*15*) to examine gene expression of sorted $CD14^+$ synovial tissue macrophages from patients with inflammatory RA ($n = 11$) and relatively noninflammatory osteoarthritis (OA; $n = 10$). Using DESeq2, we identified 509 differentially expressed genes [$\log_2$foldchange (LFC) ≥ 1, Wald adjusted P value (padj) ≤ 0.05] that were up-regulated in RA and that we defined as an "inflamed RA macrophage signature" (data file S1). This

[1]Department of Pathology, Brigham and Women's Hospital, Boston, MA, USA. [2]Harvard Medical School, Boston, MA, USA. [3]Division of Rheumatology, Inflammation and Immunity, Department of Medicine, Brigham and Women's Hospital, Boston, MA, USA. [4]Division of Pulmonary and Critical Care Medicine, Department of Medicine, Brigham and Women's Hospital, Boston, MA, USA. [5]Department of Orthopedic Surgery, Brigham and Women's Hospital, Boston, MA, USA.
*Corresponding author. Email: mbrenner@research.bwh.harvard.edu
†The individual members of the Accelerating Medicines Partnership are listed at the end of the paper.

signature contained IFN-inducible genes such as *GBP1*, *IFI6*, and *CD40*, as well as inflammatory cytokines and chemokines including *TNF*, *CCL3*, and *CXCL8*, suggesting that both IFN-induced and inflammatory transcriptional programs define the dominant macrophage state in RA. The single most significantly up-regulated gene in the inflamed RA macrophage signature was *SLAMF7* (LFC = 3.82, padj = 2.23×10^{-21}; Fig. 1A), a receptor that regulates leukocyte activation through homotypic interactions with SLAMF7 on other cells (*32*–*34*).

To validate this finding, we disaggregated synovial tissue from an independent cohort of individuals with OA ($n = 8$; 87.5% female; mean age, 67.1; range, 58 to 85) and RA ($n = 9$; 100% female; mean age, 62.1; range, 28 to 86) to quantify SLAMF7 protein expression by flow cytometry (table S1, gating in fig. S1, A to D). SLAMF7 was present at very low levels on synovial macrophages from patients with OA but was about 40-fold higher on macrophages from patients with RA (Fig. 1B; Mann-Whitney test, $P = 0.0016$). We detected SLAMF7 on up to 55% of macrophages [mean, 26.4%; 95% confidence interval (CI), 13.3 to 39.5] from patients with RA compared with less than 6% of macrophages (mean, 2.4; 95% CI, 0.35 to 4.5) from patients with OA (Fig. 1C). We were also able to obtain discarded synovial fluid from deidentified patients with RA and OA. SLAMF7 levels were twice as high on synovial fluid macrophages from patients with RA compared with OA (Fig. 1D) and on up to 48% of macrophages (mean, 24.3; 95% CI, 17.03 to 31.56) from patients with RA compared with less than 25% of macrophages (mean, 13.3; 95% CI, 6.1 to 20.5) from patients with OA (Fig. 1E). In some patients with RA, only a subset of macrophages expressed SLAMF7, whereas, in others, the majority of cells expressed this receptor (fig. S1E). In contrast, we did not observe major differences in levels of another macrophage-expressed SLAM family member, CD84 (SLAMF5) (*35*), on macrophages from synovial tissue (figs. S1F and S2, A and B) or synovial fluid (fig. S2, C and D) from patients with RA versus OA. This identifies SLAMF7 as a receptor that is selectively expressed by inflammatory macrophages in RA.

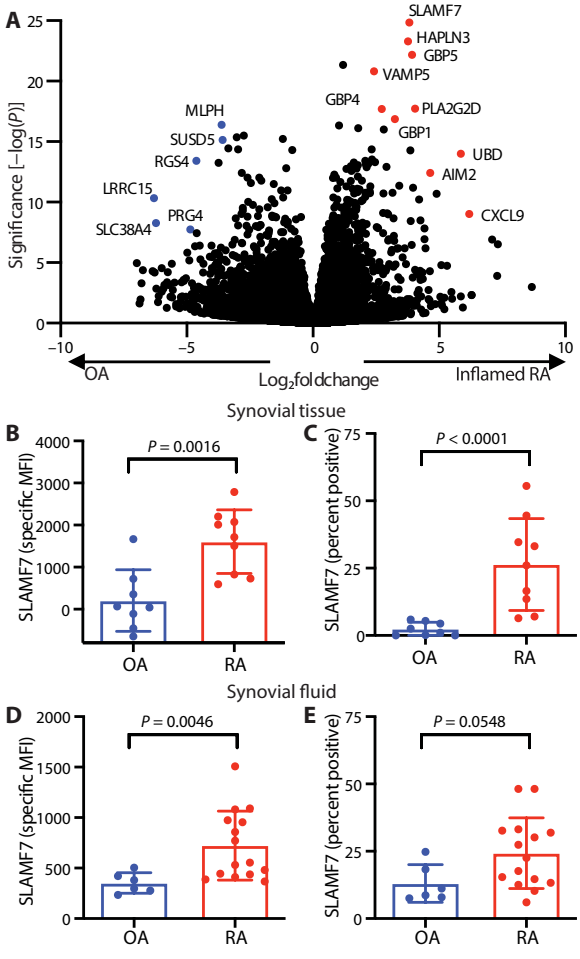

Fig. 1. Marked up-regulation of SLAMF7 on macrophages from inflamed synovial tissue. (**A**) Differential gene expression in bulk RNA-seq of synovial tissue macrophages from patients with inflamed RA ($n = 11$) compared with OA ($n = 10$) (*15*). (**B**) Specific MFI for SLAMF7 and (**C**) percent of macrophages expressing SLAMF7 in synovial tissue from patients with OA ($n = 8$) or RA ($n = 9$). (**D**) Specific MFI for SLAMF7 and (**E**) percent of macrophages expressing SLAMF7 in synovial fluid from patients with OA ($n = 6$) or RA ($n = 15$). Data represent means ± SD. Mann-Whitney test was used for statistical comparisons.

IFN-γ is a dominant driver of macrophage SLAMF7 expression

In the unstimulated state, SLAMF7 is expressed at high levels by plasma cells (*36*) and can also be expressed on B cells, T cells, and natural killer (NK) cells but is expressed at low levels on resting macrophages (*35*, *37*). However, elevated SLAMF7 expression has been found on macrophages from atherosclerotic lesions (*38*) and from patients with myelofibrosis (*39*). B lymphocyte-induced maturation protein-1 (BLIMP-1) regulates SLAMF7 expression in lymphocytes (*40*), but it is not well understood how this receptor is regulated in macrophages. We used RNA-seq to define the transcriptional activation state of macrophages with high levels of SLAMF7 by sorting $CD14^+$ and $CD16^+$ myeloid populations with high and low expression of SLAMF7 (gating in fig. S3) from peripheral blood of healthy controls (table S1: $n = 5$; 80% female; mean age, 59.6; range, 45 to 74) or patients with RA ($n = 7$; 57.1% female; mean age, 53.7; range, 37 to 67), as well as synovial fluid from patients with RA ($n = 4$; 50% female; mean age, 53.5; range, 42 to 67). We then examined genes that were differentially expressed in sorted cells with high versus low expression of SLAMF7 and identified 21 genes that were commonly up-regulated (LFC ≥ 1, padj ≤ 0.05) in $CD14^+$ populations of cells with high SLAMF7 expression from both blood and synovial fluid that we defined as a "SLAMF7-high macrophage signature" (data file S2). In addition to *SLAMF7*, IFN-inducible genes *CXCL9*, *CD40*, and *IDO1* were up-regulated in SLAMF7-high $CD14^+$ cells from blood (Fig. 2A) and synovial fluid (fig. S4A), with down-regulation of genes such as *SELL* and *SERPINB2* (Fig. 2A and fig. S4A). Gene set enrichment analysis revealed that high SLAMF7 expression was significantly associated (padj < 0.05) with Molecular Signatures Database (MSigDB) Hallmark gene sets for type I and type II IFN response (Fig. 2B), suggesting a prominent in vivo role for IFN in regulation of this receptor on macrophages. Oxidative phosphorylation pathways, which have been associated with anti-inflammatory macrophages rather than the glycolytic M1 state (*41*), were enriched in cells with high SLAMF7. TNF signaling was decreased in monocytes with high SLAMF7 (Fig. 2B). The transcription factor *EGR1*, which can suppress inflammatory gene expression (*42*), was expressed at significantly lower levels (LFC = −1.53, padj = 0.0017) in synovial fluid cells with high SLAMF7, suggesting that these cells are in a poised or potentiated but not yet fully activated state.

We then performed in vitro cytokine stimulation on monocyte-derived macrophages from peripheral blood to determine how

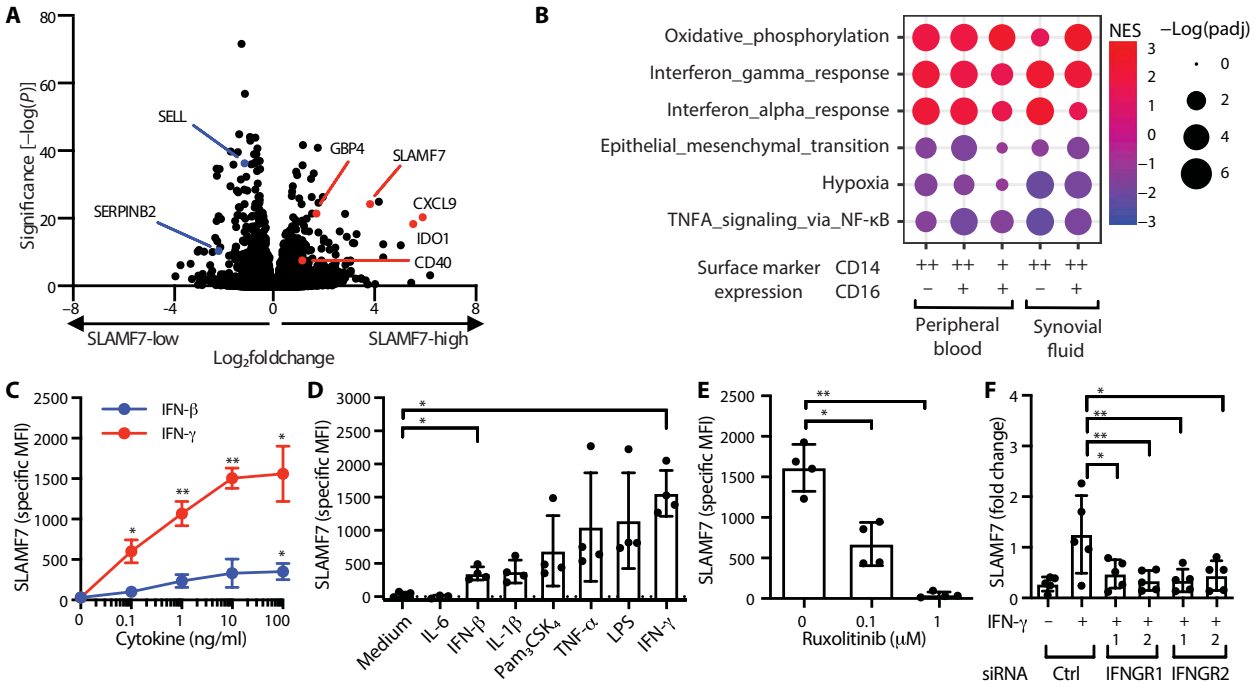

Fig. 2. SLAMF7 is a key feature of IFN-γ-potentiated macrophages. (**A**) Differential gene expression in SLAMF7-high versus SLAMF7-low $CD14^{+}CD16^{-}$ cells from peripheral blood ($n = 12$). (**B**) Gene set enrichment analysis for Hallmark pathways in SLAMF7-high compared with SLAMF7-low myeloid populations from synovial fluid and peripheral blood. (**C**) Specific MFI for SLAMF7 on macrophages incubated with different doses of IFN-γ or IFN-β. (**D**) Specific MFI for SLAMF7 on macrophages incubated with cytokines or TLR agonists (100 ng/ml). IFN-β and IFN-γ results are the same as the dose at 100 ng/ml in (C). (**E**) Macrophages were incubated with ruxolitinib (JAK inhibitor) or dimethyl sulfoxide before IFN-γ treatment (10 ng/ml), and the specific MFI for SLAMF7 was measured after 16 hours. Data in (C) to (E) represent means ± SD of four donors. (**F**) Macrophages were treated with a siRNA control or siRNA targeting *IFNGR1* or *IFNGR2* and then potentiated with IFN-γ (5 to 10 ng/ml) for 24 hours. *SLAMF7* was quantified relative to macrophages treated with control siRNA only. Data represent means ± SD of five donors. Statistics were calculated using the one-way analysis of variance (ANOVA) with Dunnett's multiple comparisons test. NES, normalized expression score; Ctrl, control; $^{*}P \leq 0.05$; $^{**}P \leq 0.01$.

SLAMF7 is regulated on macrophages. Treatment of macrophages with IFN-γ resulted in high expression of SLAMF7 (Fig. 2C). Cytokines IFN-β, IL-1β, and TNF-α, as well as TLR agonists N-palmitoyl-S-[2,3-bis(palmitoyloxy)-(2RS)-propyl]-[R]-cysteinyl-[S]- seryl-[S]-lysyl-[S]-lysyl-[S]-lysyl-[S]-lysine (Pam_3CSK_4) and lipopolysaccharide (LPS), also increased expression of SLAMF7 on macrophages but to lower levels than IFN-γ, whereas IL-6 did not affect SLAMF7 expression (Fig. 2D). In contrast, CD84 levels decreased by up to 50% after stimulation with IFN-β, IL-1β, TNF-α, Pam_3CSK_4, LPS, and IFN-γ (fig. S4, B and C), whereas CD45 levels were relatively unchanged (fig. S4, D and E). Janus kinase 1 (JAK1) and JAK2 are known to transduce IFN-γ signaling (*43*). Inhibitors of JAK1 and JAK2 such as ruxolitinib effectively disrupt this pathway and are used clinically to treat patients with myelofibrosis (*44*) and graft-versus-host disease (*45*). We observed strong inhibition of IFN-γ–induced SLAMF7 expression in macrophages treated with ruxolitinib in vitro (Fig. 2E), confirming the importance of this pathway and revealing a potential method to disrupt SLAMF7 up-regulation. Conversely, there was a doubling in CD84 expression in macrophages treated with ruxolitinib (fig. S4F), suggesting reciprocal regulation of these two SLAM family members by IFN-γ. CD45 expression was unchanged by ruxolitinib treatment (fig. S4G). Next, we used small interfering RNA (siRNA) to reduce expression of IFN-γ receptors, *IFNGR1* (fig. S4H) and *IFNGR2* (fig. S4I), which resulted in decreased *SLAMF7* levels (Fig. 2F) and further supports that IFN-γ is a key regulator of SLAMF7 expression in macrophages.

Engagement of SLAMF7 triggers an inflammatory cascade

We next asked whether the increased expression of SLAMF7 on macrophages from inflamed tissues might play a role in their activation. SLAMF7-high macrophages from blood and synovial fluid expressed higher levels of IFN-induced genes but not the inflammatory genes from the inflamed RA macrophage signature. On the basis of the up-regulation of SLAMF7 after primary IFN-γ stimulation, we hypothesized that SLAMF7 engagement might provide a specific signal to control activation of macrophages primed to up-regulate its expression. SLAMF7 has previously been reported to inhibit activation of monocytes (*46*, *47*), and we wondered whether this receptor might serve to down-regulate macrophage activation. However, silencing *SLAMF7* with siRNA did not result in increased TNF production after IFN-γ treatment (Fig. 3A and fig. S5A), despite a reduction in SLAMF7 expression (Fig. 3B and fig. S5B). Thus, we next evaluated the hypothesis that SLAMF7 may instead serve to activate IFN-γ-potentiated macrophages.

Recombinant SLAMF7 (r-SLAMF7) protein has been reported to drive proliferation of myeloma cells (*48*), so we tested the response of macrophages using this recombinant protein as a soluble ligand. First, we pretreated macrophages with IFN-γ to induce SLAMF7 up-regulation, and, second, we added r-SLAMF7 protein to engage the receptor. Macrophages exhibited a remarkable 80-fold increase in *TNF* RNA (Fig. 3C) and 30-fold increase in TNF-α protein (fig. S5C) that was significantly reduced after siRNA silencing of

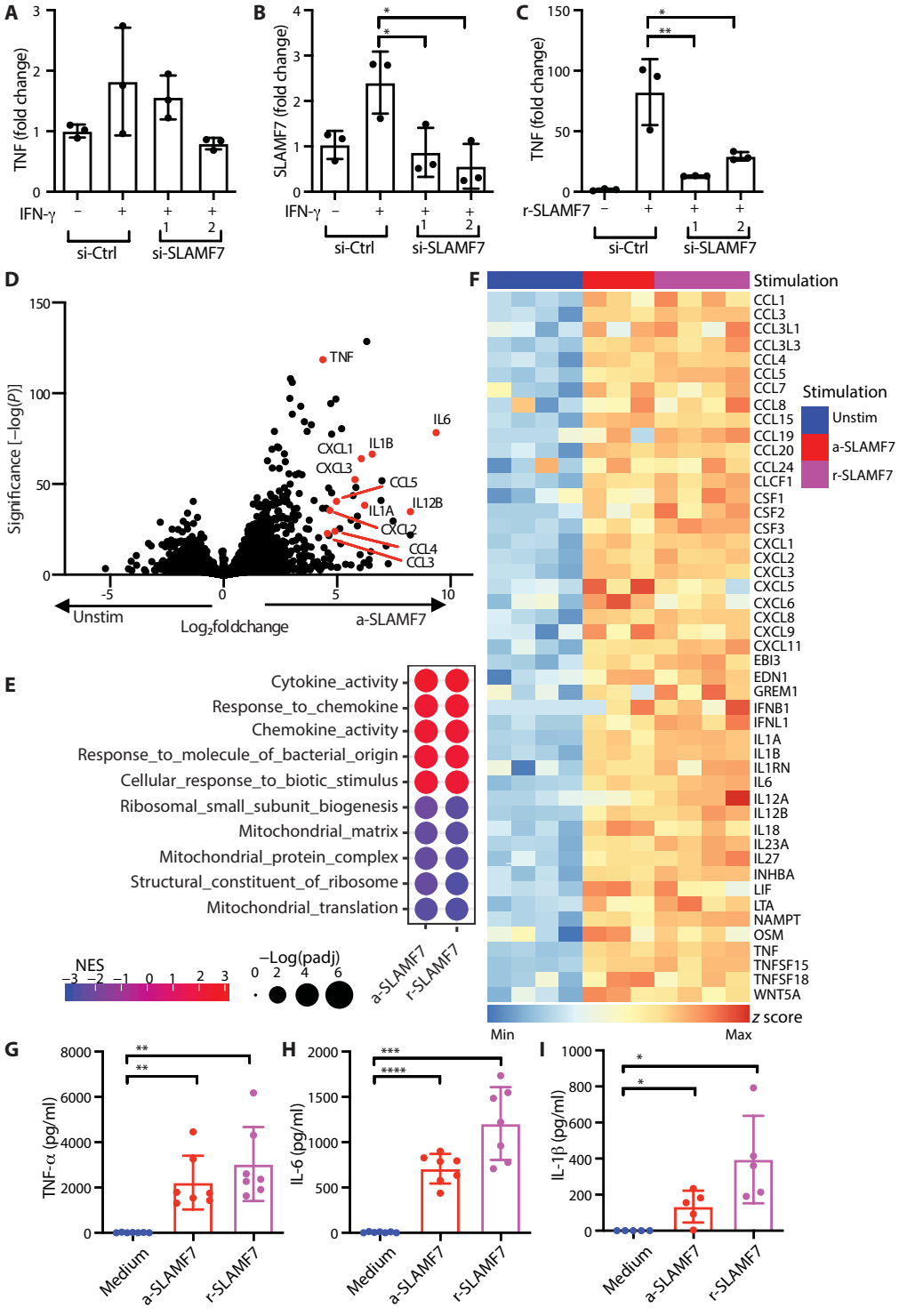

Fig. 3. Engagement of SLAMF7 triggers an inflammatory program. (**A** to **C**) Macrophages were treated with siRNA control or siRNA targeting *SLAMF7*. They were then potentiated with IFN-γ (10 ng/ml) for 24 hours. (A) *TNF* or (B) *SLAMF7* expression was quantified relative to macrophages treated with control siRNA only by RT-PCR. (C) After potentiation with IFN-γ, macrophages were stimulated with r-SLAMF7 (100 ng/ml) for 2.5 hours, and *TNF* was quantified relative to macrophages treated with control siRNA and IFN-γ only by RT-PCR. Data represent means ± SD of triplicate samples in an experiment representative of at least two independent experiments. (**D** to **I**) Macrophages were potentiated with IFN-γ (10 ng/ml) for 24 hours before treatment with a-SLAMF7 (10 μg/ml) or r-SLAMF7 (1 μg/ml) for 4 hours. (D) Differential gene expression for macrophages incubated with a-SLAMF7 ($n = 3$ donors) compared with macrophages treated with only IFN-γ ($n = 4$ donors). (E) Gene set enrichment analysis for macrophages after stimulation with a-SLAMF7 or r-SLAMF7 showing the top and bottom five GO categories for macrophages after SLAMF7 engagement. (F) Heatmap showing *z* scores for gene expression values of differentially expressed genes in the MSigDB GO:cytokine activity gene set for IFN-γ pretreated macrophages without additional stimulation ($n = 4$ donors), stimulated with a-SLAMF7 ($n = 3$ donors), or stimulated with r-SLAMF7 ($n = 4$ donors). (G) Secreted TNF-α and (H) secreted IL-6 after macrophage incubation with a-SLAMF7 or r-SLAMF7 ($n = 7$ donors). (I) Release of IL-1β after macrophage incubation with a-SLAMF7 or r-SLAMF7 for 4 hours followed by treatment with nigericin (10 μM) for 30 m ($n = 5$ donors). Data represent means ± SD. Statistics were calculated with the one-way ANOVA, using Dunnett's multiple comparisons test. Unstim, unstimulated; si-Ctrl, control siRNA; si-SLAMF7, siRNA against *SLAMF7*; $^{*}P \leq 0.05$; $^{**}P \leq 0.01$; $^{***}P \leq 0.001$; $^{****}P \leq 0.0001$.

SLAMF7 (Fig. 3C and fig. S5C). We confirmed that endotoxin levels in this protein were less than 1 endotoxin unit (EU)/ml (fig. S6A) and induced secretion of 10 to 20 times more TNF-α than other (control) protein preparations from the same company (fig. S6B), including after endotoxin depletion (fig.S6, C and D). Monocytes treated with the 162.1 SLAMF7-activating monoclonal antibody (mAb) (*32*) produced much higher levels of TNF-α than control antibodies (fig. S6F). We also evaluated endotoxin levels in and did not detect endotoxin levels within the range of the assay for this antibody and other antibodies from the same company (<0.1 EU/ml, fig. S6E). Together, these results suggest that engagement of SLAMF7 receptor can drive the notable macrophage activation that we observed.

To define transcriptome-wide changes driven by SLAMF7 engagement, we first pretreated macrophages with IFN-γ to induce high SLAMF7 expression, and, second, we used SLAMF7-activating antibody (a-SLAMF7) or r-SLAMF7 protein to engage cellular SLAMF7.

We then performed RNA-seq on these in vitro–stimulated macrophages to examine transcriptome-wide changes in gene expression (table S1: $n = 4$ donors; 100% female; mean age, 34.3; range, 22 to 70). We identified marked changes in gene expression after SLAMF7 engagement, with 596 up-regulated genes driven by both a-SLAMF7 and r-SLAMF7 (LFC ≥ 1, padj ≤ 0.05) that we defined as the "macrophage SLAMF7 stimulation signature" (data file S3). We observed up-regulation of inflammatory cytokines *TNF*, *IL1B*, *IL6*, and *IL12B* as well as chemokines *CCL3*, *CCL4*, *CXCL1*, *CXCL2*, and *CXCL8* after treatment with activating a-SLAMF7 mAb (Fig. 3D) or r-SLAMF7 protein (fig. S7A) compared with macrophages treated with IFN-γ alone. *SLAMF7* was itself up-regulated after stimulation, suggesting a positive feedback loop. In contrast, we detected down-regulation of the transcription factor *CEBPA*, which regulates monocyte development (*49*) and may inhibit inflammatory pathways in monocytes (*50*). Gene set enrichment analysis identified strong enrichment of MSigDB Gene Ontology (GO) categories (padj < 0.05) including cytokine activity and response to molecule of bacterial origin (Fig. 3E), indicating that triggering SLAMF7 drives a dominant myeloid inflammatory program. Mitochondrial and ribosomal pathways were down-regulated (Fig. 3E), suggesting changes in metabolism to support this strong inflammatory macrophage state. A large number of cytokines were up-regulated in macrophages stimulated with either a-SLAMF7 mAb or r-SLAMF7, as visualized by heatmap (Fig. 3F).

Consistent with this profoundly inflammatory state identified by RNA-seq, secreted TNF-α levels increased from 12 pg/ml to 2.2 to 3.0 ng/ml after stimulation (Fig. 3G) and IL-6 levels increased from 6 pg/ml to 0.7 to 1.2 ng/ml after stimulation (Fig. 3H). Real-time polymerase chain reaction (RT-PCR) analysis confirmed the induction of *CCL3*, *CXCL1*, and *CXCL8* after SLAMF7 engagement (fig. S7, B to D). The inflammatory cytokine *IL1B* was strongly up-regulated after stimulation with SLAMF7. However, macrophages only express high levels of inflammasome components and pro–IL-1β when they are primed by microbial TLR agonists or cytokines like TNF-α, and subsequent inflammasome activation with pyroptotic cell death is required for abrupt release of bioactive IL-1β (*31*, *51*). We detected release of IL-1β (134 to 395 pg/ml) from macrophages stimulated with SLAMF7 when nigericin was added to activate the inflammasome (Fig. 3I), suggesting that SLAMF7 can also prime inflammasomes. We also sought to verify the relevance of this pathway in cells from diseased human tissues by purifying macrophages from synovial fluid of patients with RA. Stimulation of SLAMF7 on synovial fluid macrophages with r-SLAMF7 protein resulted in strong induction of *TNF* (mean LFC = 5.0; fig. S7E) and *IL1B* (mean LFC = 6.9; fig. S7F), indicating the potential importance of this receptor in macrophage activation in RA.

We did not observe a strong overlap with the MSigDB Immunologic Signatures gene set for classically activated M1 macrophages. The "classical M1 versus alternative M2 macrophage" up-regulated gene set (*52*) defines activation after 18 hours combined stimulation with IFN-γ and LPS, but the array of cytokines driven by SLAMF7 engagement was notably absent from that signature. Other M1 activation protocols include initial priming with IFN-γ followed by LPS, which results in production of inflammatory cytokines and gene expression (*53*) that partially overlaps with those that we identified in our conditions. This underscores the fact that this SLAMF7 activation program serves as a separate step after primary stimulation of macrophages by IFN-γ or other M1 differentiation/activation factors. These sequential in vitro conditions include (i) the initial macrophage potentiation with IFN-γ to drive high SLAMF7 expression, followed by (ii) engagement of SLAMF7 and completion of activation, underscoring this distinct program. We termed this as activation state, defined by up-regulation of the SLAMF7 receptor followed by SLAMF7 engagement that then triggers profound inflammatory activation, as the SLAMF7-SAM state.

SLAMF7 drives an inflammatory signaling cascade

SLAMF7 contains a cytoplasmic immunoreceptor tyrosine switch motif that can either drive inhibitory signaling by phosphatases or can alternatively allow the docking of the adaptor Ewing's sarcoma associated transcript 2 (EAT-2) to activate downstream pathways while sterically blocking binding of inhibitory phosphatases (*54*, *55*). SLAMF7 engagement drives activation of NK cells through phospholipase C and Akt (*56*) and has been reported to activate macrophages independent of EAT-2 by recruiting the immunoreceptor tyrosine activating motif–bearing proteins Fc common gamma chain (FcγR) and DNAX activating protein of 12 kDa (DAP12) (*57*). To assess which pathways might control the activation observed in human macrophages, we first assessed the expression of EAT-2 (*SH2D1B*), FcγR (*FCER1G*), and DAP12 (*TYROBP*) in the bulk RNA-seq data for synovial tissue macrophages from the AMP cohort (*15*). We detected high levels of *FCER1G* and *TYROBP* but not *SH2D1B* in synovial macrophages (Fig. 4A). There was similar gene expression in the $CD14^+$ cells that we sorted from synovial fluid (fig. S8A) and peripheral blood (fig. S8B), suggesting that the EAT-2 adaptor is unlikely to contribute to macrophage activation through SLAMF7. We then evaluated whether activating FcγR or DAP12 contributes to activation of macrophages by SLAMF7. Silencing *FCER1G*, but not *TYROBP*, reduced production of TNF-α by macrophages after stimulation with r-SLAMF7 (Fig. 4B and fig. S8, C and D), suggesting that FcγR plays an important role in macrophage activation by SLAMF7.

We then explored activation of pathways downstream of FcγR, which signals through SYK and SRC pathways (*58*, *59*), resulting in phosphorylation of downstream mediators including rat sarcoma (RAS)/extracellular signal–regulated kinase (ERK), phosphatidylinositol 3-kinase/AKT, phospholipase C–γ, NF-κB, and MAPK pathways (*60*, *61*). Engagement of SLAMF7 with r-SLAMF7 resulted in doubling of ERK phosphorylation (Fig. 4C) and more than four times more phosphorylation of NF-κB P65 (Fig. 4D) at the time points tested. We also detected more than 10 times higher phosphorylation of MAPK P38 (Fig. 4E) and an almost threefold increase in AKT phosphorylation (Fig. 4F). This implicates SLAMF7 as a receptor that activates multiple pathways associated with macrophage metabolism to drive inflammatory gene expression.

SLAMF7 amplifies macrophage activation through a TNF-α autocrine loop

The magnitude of macrophage activation by SLAMF7 engagement was so notable that we wondered whether it might recruit autocrine amplification pathways. A time course revealed the rapid induction of *TNF* RNA in 30 min, resulting in secretion of TNF-α within 2 hours, with continued accumulation over time (Fig. 5A). On the basis of the rapid induction of TNF-α, we hypothesized that this cytokine might provide an autocrine amplification signal, as previously noted in other signaling contexts (*28*, *62*). We used siRNA to silence the genes encoding the receptors for TNFR1 (*TNFRSF1A*, fig. S9A) and

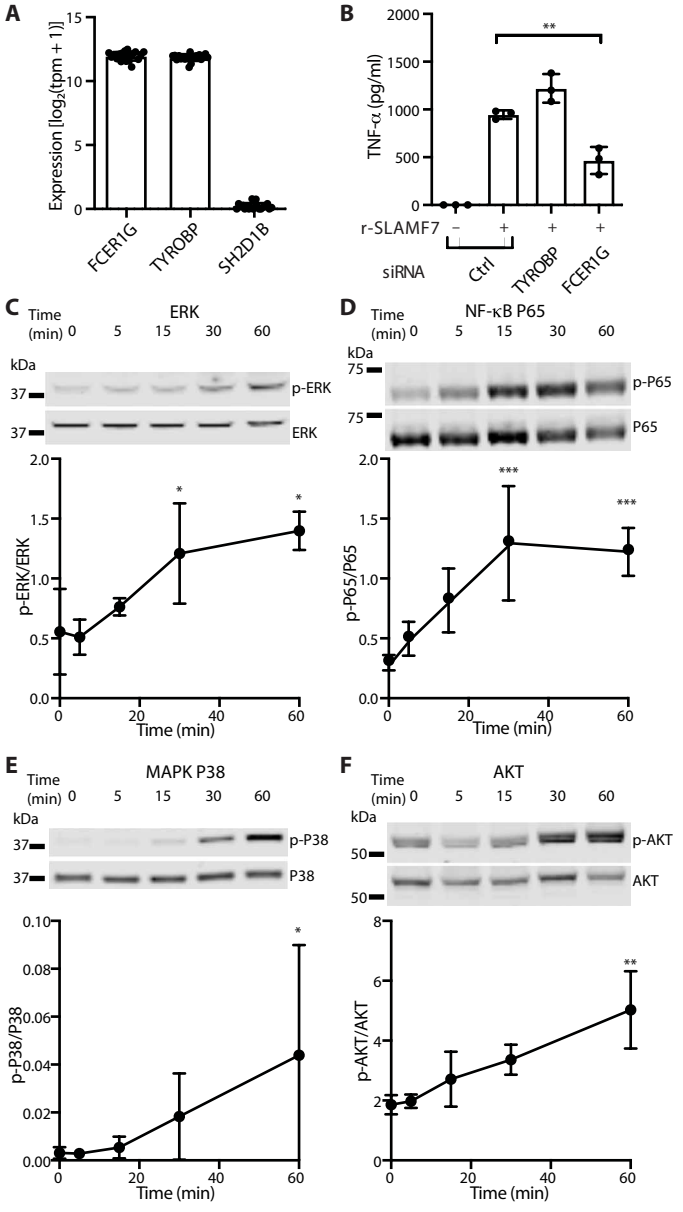

Fig. 4. SLAMF7 engagement drives an inflammatory signaling cascade. (**A**) Gene expression in bulk RNA-seq of synovial tissue macrophages from patients with arthritis from AMP ($n = 21$ donors) (*15*). (**B**) Macrophages were treated with siRNA control or siRNA targeting *TYROBP* or *FCER1G*. Cells were potentiated with IFN-γ (5 ng/ml) for 24 hours and then stimulated with r-SLAMF7 (100 ng/ml) for 4 hours. Secreted TNF-α was measured by ELISA. Data represent means ± SD of triplicate wells from an experiment representative of at least two independent experiments. (**C** to **F**) Macrophages were potentiated with IFN-γ (10 ng/ml) for 24 hours and then stimulated with r-SLAMF7 (100 ng/ml) for the times indicated. Representative Western blots and densitometry quantification for (C) ERK and phospho-ERK, (D) P65 and phospho-P65, (E) MAPK P38 and phospho-MAPK P38, and (F) AKT and phospho-AKT. Data represent means ± SD of at least three donors. Statistics were calculated using the one-way ANOVA with Dunnett's multiple comparisons test. $^*P \le 0.05$; $^{**}P \le 0.01$; $^{***}P \le 0.001$; tpm, transcripts per million.

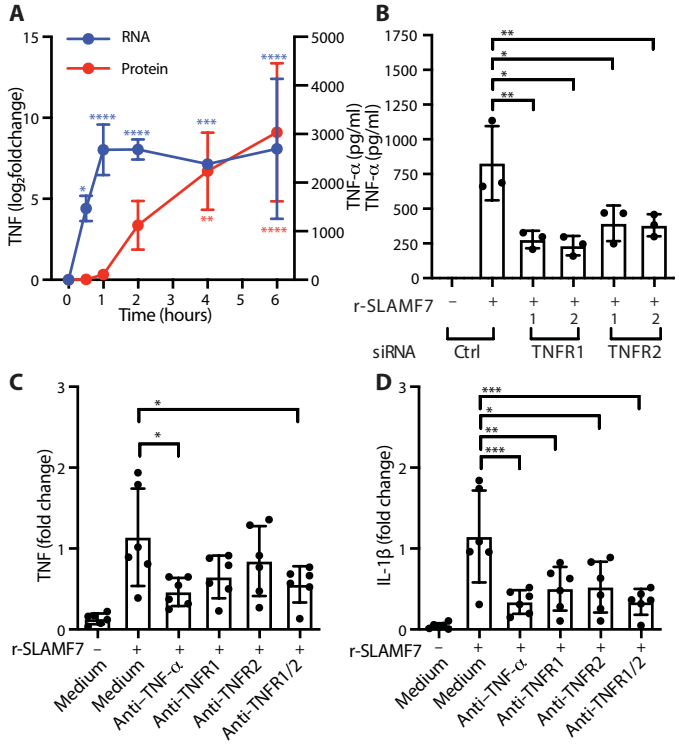

Fig. 5. SLAMF7 amplifies macrophage activation through a TNF-α autocrine loop. (**A**) Macrophages were potentiated with IFN-γ (10 ng/ml) for 24 hours and then stimulated with r-SLAMF7 (500 ng/ml). *TNF* RNA was measured at each time point relative to unstimulated cells (blue) by RT-PCR, and secreted TNF-α protein was measured by ELISA (red). Data represent means ± SD of four donors. (**B**) Macrophages were treated with siRNA control or siRNA targeting TNFR1 (*TNFRSF1A*) or TNFR2 (*TNFRSF1B*), potentiated with IFN-γ (5 ng/ml) for 16 to 18 hours, and stimulated with r-SLAMF7 (100 ng/ml) for 3 hours. TNF-α was measured by ELISA. Data represent means ± SD of triplicate wells from an experiment representative of at least three independent experiments. (**C** and **D**) Macrophages were potentiated with IFN-γ (10 ng/ml) for 24 hours, treated with antibodies for 30 min, and stimulated with r-SLAMF7 (100 ng/ml) for 8 hours. RT-PCR was used to quantify (C) *TNF* and (D) *IL1B* relative to macrophages without antibody pretreatment. Data represent means ± SD of six donors. Statistics were calculated using the one-way ANOVA with Dunnett's multiple comparisons test. $^*P \le 0.05$; $^{**}P \le 0.01$; $^{***}P \le 0.001$; $^{****}P \le 0.0001$.

TNFR2 (*TNFRSF1B*, fig. S9B), resulting in a marked reduction of TNF-α secretion after stimulation with r-SLAMF7 (Fig. 5B). Antibody blockade of TNF-α decreased expression of *TNF* (Fig. 5C) and *IL1B* (Fig. 5D) by about 50% after SLAMF7 stimulation. Corresponding blockade of the TNFR1 and TNFR2 receptors also reduced levels of *TNF* (Fig. 5C) and *IL1B* (Fig. 5D). This implicates TNF-α autocrine signaling as an additional amplification step for inflammatory pathway activation after SLAMF7 engagement in SLAMF7-SAMs.

SLAMF7 superactivation of macrophages in RA

In the data from the AMP cohort (*15*), we had observed much higher *SLAMF7* gene expression in synovial tissue macrophages from patients with RA compared with OA (Fig. 1). We then evaluated expression of the 596 genes in the macrophage SLAMF7 stimulation signature identified by in vitro stimulation of macrophages (Fig. 3) in the AMP bulk RNA-seq data by calculating the percent of gene expression derived from SLAMF7-induced genes. Expression of these genes as a "SLAMF7 activation score" was almost twice as

high in RA compared with OA (Fig. 6A), suggesting that SLAMF7-SAM program specifically contributes to RA. We also analyzed an independent single-cell RNA-seq dataset on synovial macrophages (*18*), focusing on the comparison between healthy controls and untreated patients with RA. Macrophages from patients with RA had more than double the levels of *SLAMF7* relative to healthy controls (Fig. 6B), along with increased levels of the SLAMF7 activation score (Fig. 6C). One untreated individual (SA220) with both low *SLAMF7* and the SLAMF7 activation score (Fig. 6, B and C) also had a low disease activity score compared with other patients with untreated RA in the study (*18*), suggesting that *SLAMF7* and its activation score may relate to disease activity.

We then performed clustering of macrophages from healthy controls and patients with untreated RA and visualized using uniform manifold approximation and projection (UMAP) (Fig. 6D). These cells uniformly expressed *CD14* and *CD68*, with one large population expressing *MERTK* and *FOLR2*, and another with high levels of *CD48* (fig. S10, A to C). We further subdivided these populations into groups defined by expression of *TREM2*, *LYVE1*, *CLEC10A*, *S100A12*, or *SPP1* (fig. S10, D to F). As previously reported (*18*), the *SPP1*$^+$ and *S100A12*$^+$ populations were expanded in most patients with RA (Fig. 6E). We observed prominent expression of the SLAMF7 activation score in the *SPP1*$^+$ and *S100A12*$^+$ clusters that were expanded in patients with RA (Fig. 6F). The *SPP1*$^+$ cluster had very high expression of *SLAMF7*, transcription factor *NFKB1*, and inflammatory cytokine *CXCL8* (Fig. 6G and fig. S11, A and B, red circle). This population also exhibited high levels of IFN-induced *CD40* and *GBP1*, as well as cytokines such as *TNF*, *CCL3*, and *CXCL2* (fig. S11, C to E, red circle). This suggests that the high expression of *SLAMF7*, along with its gene expression signature, represents the superactivated SLAMF7-SAMs, which may contribute to disease pathology.

SLAMF7 superactivation of macrophages in autoimmune and infectious disease

On the basis of our detection of the SLAMF7-SAM state in RA, we evaluated public data from other inflammatory diseases. Macrophages contribute to inflammatory pathways in Crohn's disease (*6*–*8*) as part of the GIMATS [immunoglobulin G (IgG) plasma cells, inflammatory mononuclear phagocytes, and activated T and stromal cells] module that has been associated with resistance to TNF-blockade in patients with IBD (*8*), and macrophages are also major contributors to pathological inflammation in individuals with COVID-19 pneumonia (*20*, *21*).

We analyzed publicly available single-cell RNA-seq data on ileal tissue from patients with Crohn's disease (*8*) and bronchoalveolar lavage fluid from individuals infected with COVID-19 (*20*) to determine whether this SLAMF7 activation program identified in RA contributes to macrophage-driven inflammation in other diseases. First, we used gene set enrichment analysis to compare the gene expression profiles of macrophages from inflamed ileal tissue and infected lungs to genes up-regulated in RA that we had defined as the inflamed RA macrophage signature (Fig. 1). We observed significant overlap of macrophage gene expression in both IBD and COVID-19 with gene expression in RA (Fig. 7A), suggesting common pathways of macrophage activation across tissues and diseases. We then compared the transcriptomes of macrophages from inflamed ileal tissue and bronchoalveolar lavage cells with the in vivo–derived SLAMF7-high macrophage signature (Fig. 2) and the in vitro–derived macrophage SLAMF7 stimulation signature (Fig. 3). We found a strong correlation between these signatures and gene expression in macrophages from inflamed gut and lung tissues (Fig. 7A). The average levels of SLAMF7 activation were more than twice as high in macrophages from

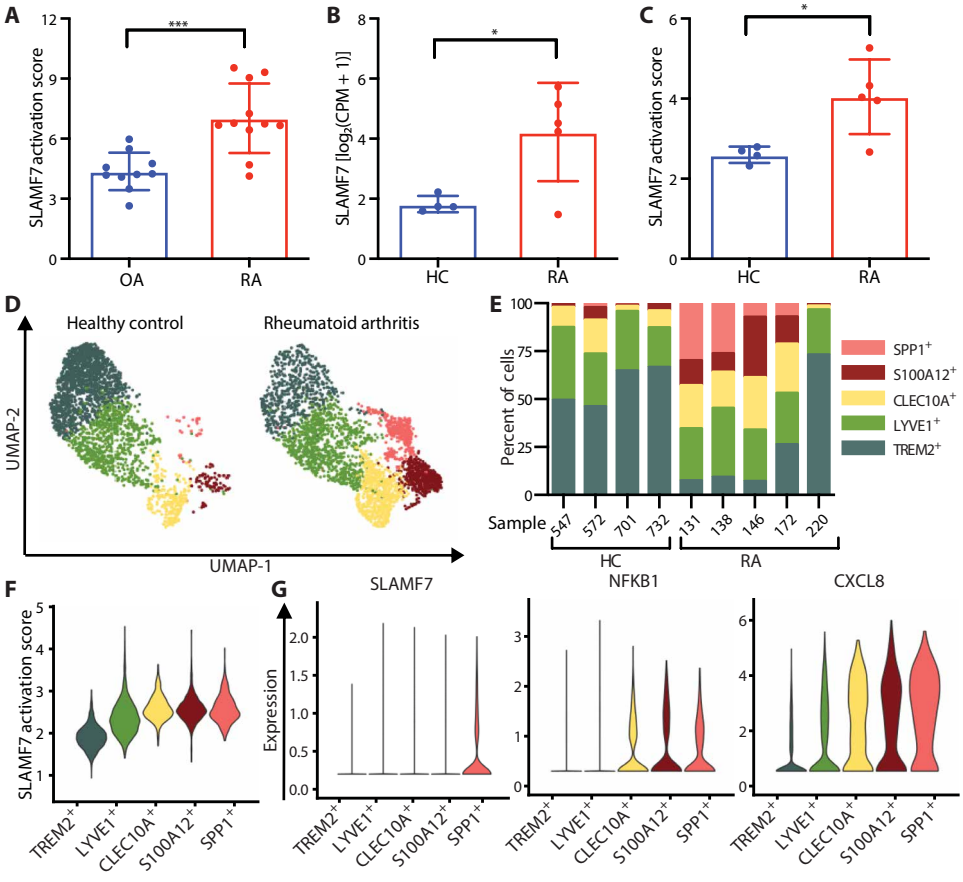

Fig. 6. SLAMF7-SAMs drive inflammation in RA. (**A**) SLAMF7 activation score for bulk RNA-seq data on synovial macrophages from patients with OA ($n = 10$) or RA ($n = 11$) (*15*). (**B**) SLAMF7 expression and (**C**) SLAMF7 activation score for pseudobulk RNA-seq data for synovial macrophages from healthy controls ($n = 4$) or patients with untreated RA ($n = 5$) (*18*). Data in (A) to (C) represent means ± SD. (**D**) UMAP plot of macrophage clusters from synovial tissues of healthy controls or patients with untreated RA. (**E**) Percent of macrophages from each donor assigned to each cluster. (**F**) Violin plot showing the SLAMF7 activation score in different macrophage populations. (**G**) Violin plots showing gene expression of synovial macrophage populations. The *t* test was used for statistical comparisons. HC, healthy control; CPM, counts per million; *$P \leq 0.05$; ***$P \leq 0.001$.

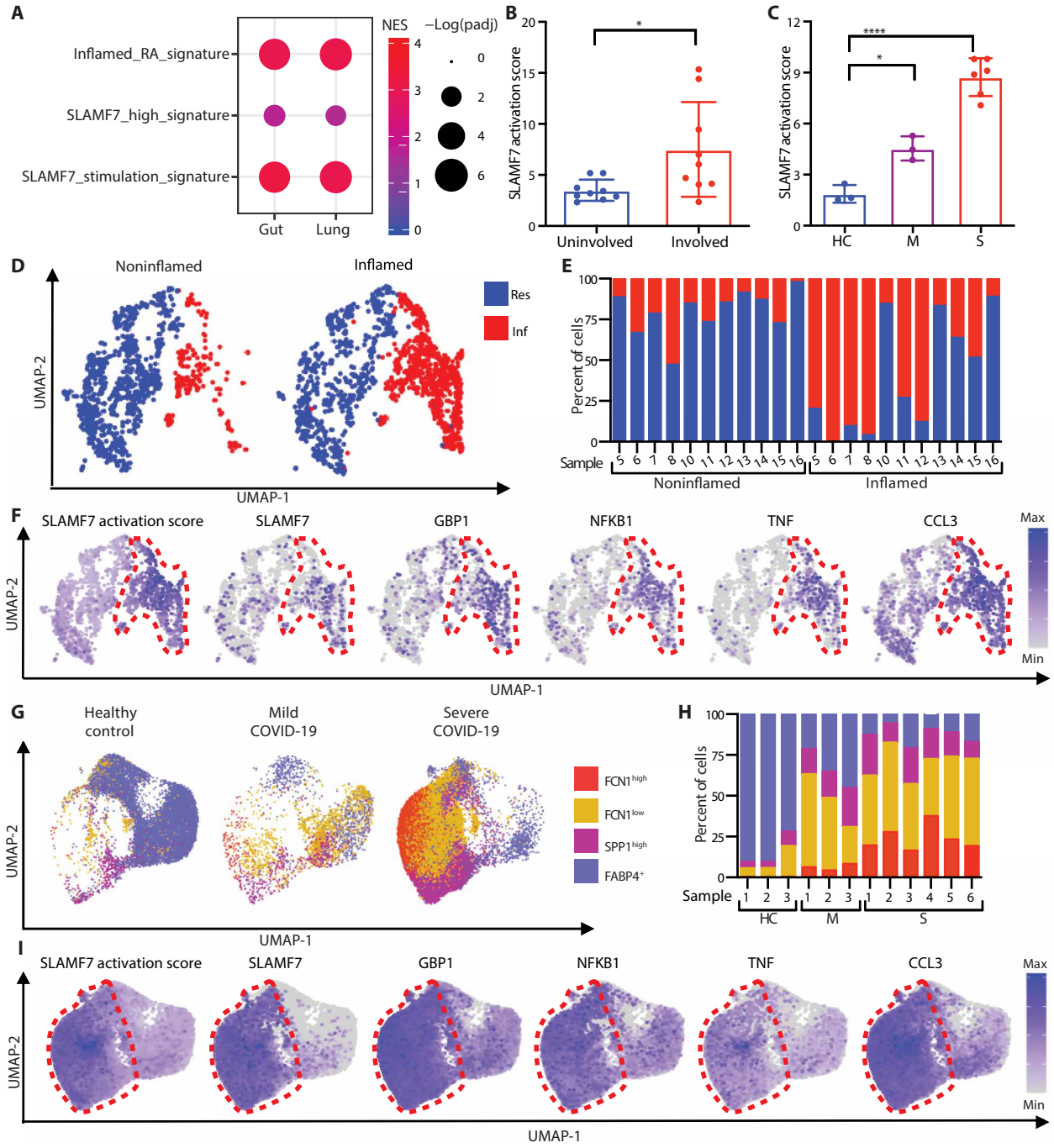

Fig. 7. SLAMF7-SAMs drive inflammation in IBD and COVID-19 infection. (**A**) Gene set enrichment analysis comparing gene expression from macrophages from inflamed ileal tissues in patients with Crohn's disease or lungs of patients with severe COVID-19 with the inflamed RA macrophage signature, the SLAMF7-high macrophage signature, and the macrophage SLAMF7 stimulation signature. (**B**) SLAMF7 activation score for macrophages from noninflamed ($n = 9$) and inflamed ileal tissues ($n = 9$) (*8*). (**C**) SLAMF7 activation score for bronchoalveolar lavage macrophages from healthy controls ($n = 3$) or individuals with mild ($n = 3$) or severe COVID-19 ($n = 6$) (*20*). Data in (B) and (C) represent means ± SD. (**D**) UMAP plot of macrophage clusters from involved and uninvolved ileal tissues. (**E**) Percent of macrophages from each donor assigned to each cluster. (**F**) UMAP plots showing gene expression of ileal macrophage populations. (**G**) UMAP plot of bronchoalveolar lavage macrophage populations. (**H**) Percent of macrophages from each donor assigned to each population. (**I**) UMAP plots showing gene expression for bronchoalveolar lavage macrophage populations. The paired *t* test was used to compare inflamed and noninflamed gut tissues, and the one-way ANOVA with Dunnett's multiple comparisons test was used to compare mild and severe COVID-19 to healthy controls. Res, resident macrophage cluster; Inf, inflammatory macrophage cluster; M, mild COVID-19; S, severe COVID-19; *$P \leq 0.05$; ****$P < 0.0001$.

inflamed gut tissue than noninflamed tissue (Fig. 7B), with the highest levels of SLAMF7 activation in samples categorized as having high rather than low GIMATS module intensity scores (fig. S12, A and B). Individuals with mild COVID-19 lung involvement had double the SLAMF7 activation levels compared with healthy controls, and the signature was more than fourfold higher in individuals with severe disease (Fig. 7C). This suggests that this SLAMF7-SAM program represents a dominant state in these inflammatory diseases.

We explored which single-cell populations displayed the SLAMF7-SAM state in vivo. First, we visualized macrophage populations from ileal tissue of patients with IBD using UMAP plots. We observed two dominant populations of ileal macrophages with expression of *CD14* and *CD68*, including a population of macrophages with higher expression of *MRC1* (fig. S13) that was present in both inflamed and noninflamed tissues, consistent with "resident macrophage" populations (Fig. 7D). Another macrophage population with higher cytokine expression was predominantly derived from inflamed tissues, consistent with "inflammatory macrophages" (Fig. 7, D and E). Gene expression from the SLAMF7 activation score was extremely high in the inflammatory macrophage population (Fig. 7F, red dotted circle). This cluster also exhibited higher expression of *SLAMF7*, as well as *GBP1*, *NFKB1*, *TNF*, *CCL3* (Fig. 7F and fig. S14, A and B), IFN-induced *CD40* and *IDO1*, and inflammatory chemokines *CXCL2* and *CXCL8* (fig. S14, C to E).

We then focused on lung macrophages from patients infected with COVID-19, including a monocyte-like $FCN1^{high}$ population, a chemokine-high $FCN1^{low}$ group, fibrosis-associated $SPP1^{high}$ macrophages (*10*), and $FABP4^{+}$ alveolar macrophages (Fig. 7G). On the UMAP plot, there was clear separation of the three $FCN1^{+}$ and $SPP1^{+}$ macrophage populations from the $FABP4^{+}$ alveolar macrophages (fig. S15), with large increases in the proportions of $FCN1^{high}$, $FCN1^{low}$, and $SPP1^{high}$ macrophage populations in individuals with COVID-19 (Fig. 7H). We observed the highest levels of the SLAMF7 activation score in cells from the $FCN1^{low}$ and $FCN1^{high}$ populations that were expanded in patients with severe disease, although it was highly expressed in all three $FCN1^{+}$ and $SPP1^{+}$ populations compared with $FAB4^{+}$ alveolar macrophages (Fig. 7I, red circle). There was also an increase in *SLAMF7* expression in $FCN1^{+}$ and $SPP1^{+}$ macrophages from patients with severe COVID-19 compared with low expression in $FABP4^{+}$ alveolar macrophages from healthy controls (Fig. 7I and fig. S16, A and B). The $FCN1^{+}$ and $SPP1^{+}$ populations also expressed high levels of *GBP1*, *NFKB1*, *TNF*, and *CCL3* (Fig. 7I and fig. S16, A and B), as well as IFN-inducible *CD40*, *IDO1*, and inflammatory *CXCL2* and *CXCL8* (fig. S16, C to E). The convergence of higher levels of *SLAMF7* and other IFN-induced genes, along with SLAMF7-induced inflammatory genes, implicates the SLAMF7-SAM state as an important factor in COVID-19 pneumonia. This macrophage activation state, defined by initial potentiation with IFN-γ and up-regulation of *SLAMF7*, followed by subsequent SLAMF7 engagement and amplification through TNF-α, is one that may play a conserved role in pathological inflammation of RA, IBD, and COVID-19 pneumonia.

DISCUSSION

Macrophages orchestrate immune responses to protect against invading microbes, but overly robust immune responses and inflammation can cause autoimmune disease or cytokine storm during infection. Here, we have identified a pathway in which SLAMF7 is a key receptor that defines a specific macrophage activation program, with the highest levels on macrophages exposed to IFN-γ and lesser but significant induction by other cytokines and TLR agonists. Subsequent triggering of SLAMF7, even in the absence of microbial molecules, drives rapid and extensive production of cytokines and chemokines that we have defined as SLAMF7-SAMs. Whereas resting macrophages are characterized by selectins and anti-inflammatory genes, IFN-γ reprograms the macrophage state, including high expression of SLAMF7. Subsequent triggering of the SLAMF7 receptor leads to production of inflammatory cytokines with autocrine amplification to drive this SLAMF7-SAM state (fig. S17). A similar inflammatory macrophage population has been reported in several single-cell RNA-seq datasets (*63*, *64*), and, here, we identify a pathway that can drive the activation of this macrophage population.

Because macrophages must pass through multiple steps to achieve this complete superactivation state, interventions targeting different parts of this pathway could allow for fine-tuned therapeutic strategies. JAK inhibitors such as ruxolitinib impair macrophage responses to IFN-γ and diminish induction of SLAMF7, thereby limiting activation of this pathway. TNF-α blockade could impair autocrine amplification of this pathway but would have limited effects on the array of inflammatory effectors driven by direct SLAMF7 stimulation. Current therapeutics targeting these pathways may partially alleviate different components driving SLAMF7-SAMs, but we did not have access to transcriptional data from treated individuals in sufficient numbers to evaluate this question in this study. The patients with inflamed RA from AMP predominantly represented not only untreated individuals but also patients treated with tofacitinib, methotrexate, and etanercept (*15*), suggesting that this macrophage state is shared across treatment conditions and is unlikely to be an effect of specific drug treatments. The absence of this receptor on normal resident macrophage populations implicates it as having particular importance as a specific target for inflammatory macrophages.

We expect that it is blockade of SLAMF7 itself that would prevent the completion of macrophage superactivation of IFN-γ–potentiated macrophages and likely have important therapeutic implications. Elotuzumab is an antibody targeting SLAMF7 that is in clinical use for treatment of relapsed multiple myeloma (*65*), and part of this drug's efficacy is through activation of NK cells (*66*) and macrophages (*67*), indicating that it has activating effects. Another antibody against SLAMF7 was used to deplete plasma cells and reduce disease severity in an animal model of arthritis (*68*), but the importance of this receptor on highly activated macrophages has not previously been appreciated. SLAMF7 and its activation signature are up-regulated in inflammatory RA, IBD, and COVID-19 pneumonia, implicating it as contributing to macrophage-driven inflammation in autoimmune and infectious diseases. Targeting this receptor and downstream pathways may offer a distinct opportunity to block severe macrophage-driven inflammation without diminishing more moderate macrophage immune surveillance and helpful homeostatic macrophage functions.

MATERIALS AND METHODS

Study design

The objective of this study was to identify receptors that regulate macrophage activation in inflammatory human disease. We analyzed publicly available RNA-seq data to identify genes that are

selectively expressed in macrophages from inflamed tissues, identifying and validating that SLAMF7 is highly expressed in synovial tissue macrophages from inflamed RA tissues. To define the transcriptional state of macrophages with high SLAMF7, we sorted myeloid cells with high versus low expression of SLAMF7. We used in vitro stimulation assays to identify IFN-γ as a dominant driver of SLAMF7 expression. We then engaged this receptor on monocyte-derived macrophages in vitro and defined a strong inflammatory gene expression signature driven by SLAMF7. We used siRNA and Western blots to define signaling pathways that drive this signature, as well as blocking antibodies to implicate a TNF-α autocrine loop that amplifies this superactivation state. Last, we analyzed other datasets to identify this SLAMF7-activated macrophage state in single-cell RNA-seq data not only from synovial tissue macrophages from patients with arthritis but also from gut macrophages from patients with IBD and lung macrophages from individuals with COVID-19 pneumonia.

Human research

Human subject research was performed with approval from the Institutional Review Board at the Brigham and Women's Hospital. Patients with RA were defined according to the American College of Rheumatology 2010 Rheumatoid Arthritis classification criteria (*69*). Synovial tissue samples were obtained as excess samples from patients undergoing arthroplasty procedures at the Brigham and Women's Hospital, and samples were frozen in Cryostor CS10 preservation medium (Sigma-Aldrich). Synovial fluid samples were obtained sterile before arthrotomy as discarded samples from routine clinical care, and peripheral blood samples were collected as discarded samples from routine clinical care. Patient consent for genomic studies was obtained for all samples used for RNA-seq.

Sample processing

Synovial tissue was disaggregated as previously described (*11*, *70*). Frozen synovial tissue was thawed and minced into small pieces that were digested with Liberase TL (100 μg/ml; Sigma-Aldrich) and deoxyribonuclease I (100 μg/ml; Sigma-Aldrich) at 37°C for 30 min. Samples were passed over a 70-μm cell strainer (Thermo Fisher Scientific), red blood cells were lysed with ammonium-chloride-potassium (ACK) lysis buffer (Thermo Fisher Scientific), and cells were stained for flow cytometry. Synovial fluid and peripheral blood were isolated as previously reported (*14*), with density centrifugation on a Ficoll-Hypaque gradient to isolate mononuclear cells. Cells were cryopreserved for subsequent analysis.

Reagents and antibodies

Recombinant human macrophage colony-stimulating factor (M-CSF), IFN-β, IFN-γ, IL-1β, IL-6, and TNF-α were from PeproTech. Enzyme-linked immunosorbent assay (ELISA) kits for TNF-α, IL-6, and IL-1β were from R&D Systems. Endotoxin quantification kits and endotoxin removal kits were from Pierce. Pam_3CSK_4 and LPS were from InvivoGen. Ruxolitinib was from Selleckchem. Nigericin was from InvivoGen. Fetal bovine serum (FBS) was from HyClone. Propidium iodide was from BioLegend, and a fixable blue dead cell stain kit was from Thermo Fisher Scientific. The following 6x-His–tagged recombinant proteins, expressed in human embryonic kidney 293 cells, with at least 95% purity, were from Sigma-Aldrich: SLAMF7 (r-SLAMF7), CD84 (r-CD84), and CD326 (r-CD326). Purified a-SLAMF7 (162.1) anti–TNF-α (MAb1), anti-CD4 (OKT4), and mouse IgG2b, κ isotype control (MPC-11) were from BioLegend. Anti-TNFR1 (16803) and anti-TNFR2 (22210) were from R&D Systems. The following antibodies were used for flow cytometry and cell sorting: CD16 (CB16, eBioscience), CD45 (HI30, BioLegend), CD14 (61D3, eBioscience), SLAMF7 (162.1, BioLegend), CD84 (CD84.1.21, BioLegend), CD3 (UCHT1, eBioscience), CD19 (HIB19, eBioscience), CD56 (CMSSB, eBioscience), TNF-α (Mab11, BioLegend), mouse IgG2b, and κ isotype control (MPC-11, BioLegend). The following antibodies from Cell Signaling Technology were used for Western blot: Akt (40D4), phospho-Akt (Ser^{473}, D9E), ERK1/2 (3A7), phospho-ERK1/2 (Thr^{202}/Tyr^{204}, D13.14.4E), p38 MAPK (polyclonal, no. 9212), phospho-p38 MAPK (Thr^{180}/Tyr^{182}, 28B10), NF-κB p65 (L8F6), and phospho–NF-κB p65 (Ser^{636}, 93H1). Fluorescent secondary antibodies anti-rabbit IRDye 680RD and anti-mouse IRDy3 800CW were from LI-COR.

Cell culture and stimulation

Monocytes were magnetic-activated cell sorting–purified from peripheral blood mononuclear cells using CD14 microbeads (Miltenyi Biotec). A total of 50,000 cells per well were cultured in flat bottom 96-well plates, or 300,000 cells per well were cultured in 24-well plates in RPMI 1640 (Thermo Fisher Scientific) with 10% FBS, with additives of β-mercaptoethanol, sodium pyruvate, Hepes, penicillin/streptomycin, L-glutamine (Thermo Fisher Scientific), and M-CSF (20 ng/ml). Macrophages were allowed to rest for at least 24 hours. Cytokines were then added for an additional 24 hours. For inhibitor experiments, ruxolitinib or an equivalent concentration of dimethyl sulfoxide was added 30 min before IFN-γ. For SLAMF7 stimulation, after 24 hours of incubation with IFN-γ, macrophages were treated with a-SLAMF7 antibody or r-SLAMF7 protein. For blocking experiments, antibodies were added at 10 μg/ml (TNFR1 and TNFR2) or 20 μg/ml (TNF-α) 30 min before stimulation with r-SLAMF7.

Small interfering RNA

Monocytes were cultured in RPMI 1640 with 10% FBS and M-CSF (20 ng/ml). They were transfected with either a control siRNA or siRNA against a gene of interest (Silencer Select, Life Technologies) at 25 to 30 nM by reverse transfection using RNAiMax (Life Technologies). After 24 to 72 hours of siRNA treatment, macrophages were treated with IFN-γ for 16 to 24 hours before analysis or stimulation with r-SLAMF7 protein.

Quantitative RT-PCR

Primers (table S2) were from Integrated DNA Technologies. RNA was processed using the RNEasy Mini kit (Qiagen) and Quantitect Reverse Transcription kit (Qiagen). RT-PCR was performed using SybrGreen (Agilent) on the AriaMX (Agilent). Gene expression for each sample was normalized to *GAPDH* and compared across conditions.

Cell staining

Cells were washed with staining buffer (phosphate-buffered saline, 2% FBS, 2 mM EDTA) (Thermo Fisher Scientific), treated with Human Trustain FcX (BioLegend) for 10 min on ice, and stained with antibodies for 30 min on ice. Propidium iodide (1 μg/ml) was added 15 min before acquisition. For stimulation experiments, cells were stained and then fixed in 4% paraformaldehyde for 10 min on ice before acquisition. The Tru-Nuclear Transcription Factor Buffer Set (BioLegend) was used for intracellular cytokine staining. Analysis was done on the LSRFortessa (BD Biosciences).

Flow cytometry analysis

Analysis was performed by gating on myeloid cells by forward scatter and side scatter, excluding doublets, and gating on $CD45^+$ leukocytes with exclusion of dead cells. $CD14^+$ cells were selected for analysis (fig. S1, A to D). Specific mean fluorescence intensity (MFI) was determined by subtracting the MFI from an isotype control from the MFI for a specific antibody. Percent positive cells were calculated by setting a gate with ≤1% of cells in a sample stained with isotype control as the threshold for positivity.

Cell sorting

Sorting was performed on a FACSAria Fusion sorter (BD Biosciences). Myeloid cells were gated as $CD45^+$ cells with exclusion of live/dead dye, CD3, CD19, and CD56. SLAMF7-low cells were defined as 40% of myeloid cells with lowest expression of SLAMF7. SLAMF7-high cells were defined as those with staining above the level of isotype control. Three populations from blood and two populations from synovial fluid were sorted on the basis of expression of CD14 and CD16 (fig. S3). Up to 1000 cells from each population were collected in Eppendorf tubes with 5 μl of TurboCapture Lysis buffer (Qiagen) (TCL) buffer and 1% β-mercaptoethanol. Cell lysates were frozen at −80°C for further processing.

Western blot

Monocytes were cultured in M-CSF, treated with IFN-γ for 16 to 24 hours, and stimulated with r-SLAMF7 protein. Cells were lysed in radioimmunoprecipitation assay buffer (Cell Signaling Technology) with 1 mM phenylmethylsulfonyl fluoride (Cell Signaling Technology) and protease/phosphatase inhibitor (Cell Signaling Technology) and boiled at 95°C in Laemmli buffer (Bio-Rad). Protein was quantified with bicinchoninic acid (BCA) (Pierce Technologies), and 25 to 50 μg of protein was loaded in each well for SDS–polyacrylamide gel electrophoresis separation (Invitrogen). Samples were transferred to nitrocellulose membrane (iBlot2, Invitrogen) for detection with primary antibodies. Fluorescent secondary antibodies were used for detection, and membranes were imaged on a LI-COR Odyssey Blot Imager (LI-COR Biotechnology). Blots were processed and analyzed with LI-COR Image Studio version 4.0.21.

RNA sequencing

Cell lysates were collected in TCL buffer with 0.1% β-mercaptoethanol and frozen at −80°C. Samples were sequenced at the Broad Institute using the Smart-seq2 RNA-seq platform (*71*–*73*). This platform uses paired read sequencing and provides around 4 million reads per sample. Samples with detection of at least 10,000 genes were used for subsequent analysis.

Analysis of bulk RNA-seq from synovial tissue macrophages

FASTQ files for bulk RNA-seq data were obtained for sorted $CD14^+$ synovial macrophages from patients with OA (n = 10) and inflamed RA (n = 11) from AMP (dbGaP phs001457.v1.p1) (*15*). Reads were quantified using kallisto. To focus on signaling receptors, we selected genes with the "protein_coding" Ensembl biotype with at least one count across samples, resulting in 18,304 genes for analysis. DESeq2 was used for differential gene expression analysis comparing macrophages from inflamed RA and OA, including both disease status and processing batch in the model. The 509 genes with LFC ≥ 1 and padj ≤ 0.05 for RA compared with OA were considered significantly up-regulated genes, defined as the inflamed RA macrophage signature (data file S1).

Analysis of bulk RNA-seq from sorted SLAMF7-high and SLAMF7-low cells

RNA-seq on SLAMF7-high and SLAMF7-low cells sorted from peripheral blood from healthy controls (n = 5) or patients with RA (n = 7) and synovial fluid from patients with RA (n = 4 donors) was performed at the Broad Institute using Smart-seq2 with 25–base pair (bp) paired reads. Read quantification was performed using the Broad Institute pipeline, with alignment to GRCh38.83 using STAR version 2.4.2a (*74*) and quantification with RSEM version 1.2.2.1 (*75*). A total of 37,414 genes were included for analysis. DESeq2 was used to calculate differential gene expression between SLAMF7-high and SLAMF7-low cells for each population, including both SLAMF7 expression and donors in the model. Genes with LFC ≥ 1 and padj ≤ 0.05 were considered significantly up-regulated, and the SLAMF7-high macrophage signature was defined as 21 genes that were up-regulated in SLAMF7-high compared with SLAMF7-low $CD14^+$ $CD16^-$ cells from both peripheral blood and synovial fluid (data file S2). Differentially expressed genes from SLAMF7-high versus SLAMF7-low cells from each population in peripheral blood and synovial fluid were ordered by the Wald statistic calculated by DESeq2. The fgsea package was used for gene set enrichment analysis with 10^6 permutations for comparison of these ordered genes to MSigDB Hallmark gene sets (h.all.v7.0.symbols.gmt).

Analysis of bulk RNA-seq from in vitro SLAMF7–stimulated macrophages

For analysis of macrophages after in vitro SLAMF7 stimulation (n = 4 donors), RNA-seq was performed using Smart-seq2 with 50-bp paired reads. Reads were quantified using kallisto. One sample stimulated with a-SLAMF7 was excluded due to low gene counts. A total of 36,513 genes were included for analysis. DESeq2 was used for differential gene expression analysis comparing macrophages potentiated with IFN-γ, followed by stimulation with either a-SLAMF7 or r-SLAMF7 to macrophages treated with IFN-γ without additional stimulation. Fold-change values were shrunk using the apeglm algorithm (*76*). Genes with LFC ≥ 1 and padj ≤0.05 were considered significantly up-regulated. The "macrophage SLAMF7 stimulation score" was defined as 596 genes that were commonly up-regulated with both a-SLAMF7 and r-SLAMF7 stimulation (data file S3). Differentially expressed genes from macrophages stimulated with a-SLAMF7 or r-SLAMF7 compared with unstimulated macrophages were ordered by the Wald statistic calculated by DESeq2. The fgsea package was used for gene set enrichment analysis with 10^6 permutations for MSigDB GO gene sets (c5.all.v7.0.symbols.gmt), and CollapsePathways was used to combine overlapping GO categories to identify top and bottom pathways.

Analysis of single-cell RNA-seq on synovial macrophages from individuals with RA

Read count matrices and metadata for single-cell RNA-seq for synovial tissue from patients with RA (E-MTAB-8322) (*18*) were downloaded on 13 July 2020. Harmony reduction was used to correct for differences between donors for clustering and UMAP analysis. Macrophages were selected for analysis based on expression of *CD68* and *CD14*, excluding possible doublets using *CD2* and *CD3D* to identify T cells, *COL1A1* and *PDPN* to identify stromal cells, and *VWF* and *CD34* to identify endothelial cells. Further subclustering was performed only on macrophages from healthy controls and individuals with untreated RA, using harmony reduction to correct

for differences between donors for clustering and UMAP analysis. There was clear separation of macrophages expressing *MERTK* and *FOLR2* versus *CD48*. These included subpopulations with *MERTK*, *FOLR2*, and *TREM2* (*TREM2*$^+$); *MERTK*, *FOLR2*, and *LYVE1* (*LYVE1*$^+$); *CD48* and *CLEC10A* (*CLEC10A*$^+$); *CD48* and *S100A12* (*S100A12*$^+$); and *CD48* and *SPP1* (*SPP1*$^+$) expression.

Analysis of single-cell RNA-seq on macrophages from ileal samples from individuals with Crohn's disease

Read count matrices for single-cell RNA-seq of ileal biopsies from patients with IBD (GSE134809) (*8*) were downloaded on 10 December 2019. Cells were filtered to include those with >500 and <5000 genes and <25% mitochondrial RNA. Harmony reduction was used to correct for differences between samples for clustering and UMAP analysis. Myeloid cells were selected for analysis based on expression of *CD68* and *CD14*. From the myeloid population, we excluded nonmacrophage populations of dendritic cells (DCs) and other cells to focus our analysis on macrophages, using *CD1C* and *FCER1A* to identify CD1c$^+$ DCs and monocyte-derived DCs, *CLEC9A* and *BATF3* to identify CD141$^+$ DCs, *CCR7* and *LAMP3* to identify migratory DCs, *GZMB* and *IRF7* to identify plasmacytoid DCs, and *CD3D* and *IGHG1* to exclude possible doublets. The remaining macrophages were positive for *CD14*, *CD68*, *CSF1R*, and *MAFB*. A cluster of resident macrophages had higher expression of *MRC1*, *CD163*, and *MERTK*, whereas a cluster of inflammatory macrophages had high expression of inflammatory cytokines and chemokines including *TNF* and *CCL3* (*8*). As described in the original publication, samples from donor 6 were excluded from additional analysis because of the low number of cells, and samples from donor 16 were excluded due to similarity in cells from involved and uninvolved tissues.

Analysis of single-cell RNA-seq from bronchoalveolar lavage of individuals with COVID-19 infection

Read count matrices for single-cell RNA-seq of bronchoalveolar lavage cells from patients with COVID-19 (GSE145926) (*20*) were downloaded on 5 May 2020, and metadata provided by the authors was downloaded from github on 21 May 2020. Myeloid cells and populations in the metadata were used as originally described for analysis (*20*). Cells were filtered to include those with >500 and <5000 genes. Harmony reduction was used to correct for differences between donors for UMAP visualization.

Custom gene set enrichment analysis

For single-cell datasets, the sum of counts for each gene from all cells for each sample was combined to generate pseudobulk RNA-seq counts. For ileal macrophages from GSE134809, DESeq2 was used for differential gene expression comparing inflamed tissues (n = 9) compared with noninflamed tissues (n = 9), including both disease involvement and donor in the model. For bronchoalveolar lavage macrophages from GSE145926, DESeq2 was used for differential gene expression comparing healthy controls (n = 3) to patients with severe COVID-19 infection (n = 6), including disease state in the model. Differentially expressed genes for macrophages from inflamed versus noninflamed tissues from patients with RA or IBD, or healthy versus COVID-19–infected individuals, were ordered by the Wald statistic calculated by DESeq2. Genes from the inflamed RA macrophage signature, the SLAMF7-high macrophage signature, and macrophage SLAMF7 stimulation signature were compiled into a custom-derived gmt file. The fgsea package was used with 10^6 permutations for gene set enrichment analysis of these ordered gene lists against these custom gene sets.

SLAMF7 activation score

The SLAMF7 activation score was calculated using the up-regulated genes (LFC $\geq$ 1, padj $\leq$0.05, n = 596 genes) from the macrophage SLAMF7 stimulation signature. For bulk RNA-seq data on CD14$^+$ synovial macrophages from AMP, the SLAMF7 activation score was calculated as the sum of counts for these 596 genes as a percent of total gene counts for each donor. For single-cell RNA-seq data on macrophages from patients with RA, IBD, or COVID-19, the SLAMF7 activation score was calculated as the sum of counts for these 596 genes as a percent of total gene counts for each cell, and the median value for all cells from each donor was used for pseudobulk analysis.

Data and statistical analysis

Flow cytometry data were analyzed using Flowjo version 10.4 (BD, Biosciences). Graphical and statistical analysis was done in RStudio version 1.1.383 with R version 3.6.0, JMP Pro version 13.0.0 (JMP Inc.), and Prism version 6.0.h (GraphPad). Kallisto version 0.46.0 was used for quantification of RNA-seq reads (*77*) using version GRCh38.97 of the Ensembl transcriptome (downloaded on 13 August 2019). Differential gene expression analysis was performed using DESeq2 version 1.24.0 (*78*). Gene set enrichment analysis was performed with fgsea version 1.10.1 (*79*) using MSigDB gene sets (downloaded on 4 December 2019), including Hallmark gene sets (h.all.v7.0.symbols.gmt), GO gene sets (c5.all.v7.0.symbols.gmt), and Immunologic Signatures gene sets (c7.all.v7.0.symbols.gmt). Heatmaps were generated using pheatmap version 1.0.12. Single-cell RNA-seq analysis was performed on a cloud computing cluster using R version 3.5.3, Seurat version 3.1.4 (*80*, *81*), and harmony version 1.0 (*82*).

SUPPLEMENTARY MATERIALS

www.science.org/doi/10.1126/sciimmunol.abf2846
Figs. S1 to S17
Tables S1 and S2
Data files S1 to S4

View/request a protocol for this paper from *Bio-protocol*.

REFERENCES AND NOTES

1. C. Shi, E. G. Pamer, Monocyte recruitment during infection and inflammation. *Nat. Rev. Immunol.* **11**, 762–774 (2011).
2. C. Nathan, A. Ding, Nonresolving Inflammation. *Cell* **140**, 871–882 (2010).
3. D. Mulherin, O. Fitzgerald, B. Bresnihan, Synovial tissue macrophage populations and articular damage in rheumatoid arthritis. *Arthritis Rheum.* **39**, 115–124 (1996).
4. A. V. Misharin, C. M. Cuda, R. Saber, J. D. Turner, A. K. Gierut, G. K. Haines, S. Berdnikovs, A. Filer, A. R. Clark, C. D. Buckley, G. M. Mutlu, G. R. S. Budinger, H. Perlman, Nonclassical Ly6C(-) monocytes drive the development of inflammatory arthritis in mice. *Cell Rep.* **9**, 591–604 (2014).
5. B. Smiljanovic, A. Grützkau, T. Sörensen, J. R. Grün, T. Vogl, M. Bonin, P. Schendel, B. Stuhlmüller, A. Claussnitzer, S. Hermann, S. Ohrndorf, K. Aupperle, M. Backhaus, A. Radbruch, G. R. Burmester, T. Häupl, Synovial tissue transcriptomes of long-standing rheumatoid arthritis are dominated by activated macrophages that reflect microbial stimulation. *Sci. Rep.* **10**, 7907 (2020).
6. N. R. West, A. N. Hegazy, B. M. J. Owens, S. J. Bullers, B. Linggi, S. Buonocore, M. Coccia, D. Görtz, S. This, K. Stockenhuber, J. Pott, M. Friedrich, G. Ryzhakov, F. Baribaud, C. Brodmerkel, C. Cieluch, N. Rahman, G. Müller-Newen, R. J. Owens, A. A. Kühl, K. J. Maloy, S. E. Plevy; Oxford IBD Cohort Investigators, S. Keshav, S. P. L. Travis, F. Powrie, Oncostatin M drives intestinal inflammation and predicts response to tumor necrosis factor-neutralizing therapy in patients with inflammatory bowel disease. *Nat. Med.* **23**, 579–589 (2017).

7. C. S. Smillie, M. Biton, J. Ordovas-Montanes, K. M. Sullivan, G. Burgin, D. B. Graham, R. H. Herbst, N. Rogel, M. Slyper, J. Waldman, M. Sud, E. Andrews, G. Velonias, A. L. Haber, K. Jagadeesh, S. Vickovic, J. Yao, C. Stevens, D. Dionne, L. T. Nguyen, A.-C. Villani, M. Hofree, E. A. Creasey, H. Huang, O. Rozenblatt-Rosen, J. J. Garber, H. Khalili, A. N. Desch, M. J. Daly, A. N. Ananthakrishnan, A. K. Shalek, R. J. Xavier, A. Regev, Intra- and inter-cellular rewiring of the human colon during ulcerative colitis. *Cell* **178**, 714–730.e22 (2019).
8. J. C. Martin, C. Chang, G. Boschetti, R. Ungaro, M. Giri, J. A. Grout, K. Gettler, L.-S. Chuang, S. Nayar, A. J. Greenstein, M. Dubinsky, L. Walker, A. Leader, J. S. Fine, C. E. Whitehurst, M. L. Mbow, S. Kugathasan, L. A. Denson, J. S. Hyams, J. R. Friedman, P. T. Desai, H. M. Ko, I. Laface, G. Akturk, E. E. Schadt, H. Salmon, S. Gnjatic, A. H. Rahman, M. Merad, J. H. Cho, E. Kenigsberg, Single-cell analysis of Crohn's disease lesions identifies a pathogenic cellular module associated with resistance to anti-TNF therapy. *Cell* **178**, 1493–1508.e20 (2019).
9. P. A. Reyfman, J. M. Walter, N. Joshi, K. R. Anekalla, A. C. McQuattie-Pimentel, S. Chiu, R. Fernandez, M. Akbarpour, C.-I. Chen, Z. Ren, R. Verma, H. Abdala-Valencia, K. Nam, M. Chi, S. Han, F. J. Gonzalez-Gonzalez, S. Soberanes, S. Watanabe, K. J. N. Williams, A. S. Flozak, T. T. Nicholson, V. K. Morgan, D. R. Winter, M. Hinchcliff, C. L. Hrusch, R. D. Guzy, C. A. Bonham, A. I. Sperling, R. Bag, R. B. Hamanaka, G. M. Mutlu, A. V. Yeldandi, S. A. Marshall, A. Shilatifard, L. A. N. Amaral, H. Perlman, J. I. Sznajder, A. C. Argento, C. T. Gillespie, J. Dematte, M. Jain, B. D. Singer, K. M. Ridge, A. P. Lam, A. Bharat, S. M. Bhorade, C. J. Gottardi, G. R. S. Budinger, A. V. Misharin, Single-cell transcriptomic analysis of human lung provides insights into the pathobiology of pulmonary Fibrosis. *Am. J. Respir. Crit. Care Med.* **199**, 1517–1536 (2019).
10. C. Morse, T. Tabib, J. Sembrat, K. L. Buschur, H. T. Bittar, E. Valenzi, Y. Jiang, D. J. Kass, K. Gibson, W. Chen, A. Mora, P. V. Benos, M. Rojas, R. Lafyatis, Proliferating SPP1/MERTK-expressing macrophages in idiopathic pulmonary fibrosis. *Eur. Respir. J.* **54**, 1802441 (2019).
11. F. Mizoguchi, K. Slowikowski, K. Wei, J. L. Marshall, D. A. Rao, S. K. Chang, H. N. Nguyen, E. H. Noss, J. D. Turner, B. E. Earp, P. E. Blazar, J. Wright, B. P. Simmons, L. T. Donlin, G. D. Kalliolias, S. M. Goodman, V. P. Bykerk, L. B. Ivashkiv, J. A. Lederer, N. Hacohen, P. A. Nigrovic, A. Filer, C. D. Buckley, S. Raychaudhuri, M. B. Brenner, Functionally Distinct Disease-Associated Fibroblast Subsets in Rheumatoid Arthritis. *Nat. Commun.* **9**, 789 (2018).
12. A. P. Croft, J. Campos, K. Jansen, J. D. Turner, J. Marshall, M. Attar, L. Savary, C. Wehmeyer, A. J. Naylor, S. Kemble, J. Begum, K. Dürholz, H. Perlman, F. Barone, H. M. McGettrick, D. T. Fearon, K. Wei, S. Raychaudhuri, I. Korsunsky, M. B. Brenner, M. Coles, S. N. Sansom, A. Filer, C. D. Buckley, Distinct fibroblast subsets drive inflammation and damage in arthritis. *Nature* **570**, 246–251 (2019).
13. D. Kuo, J. Ding, I. S. Cohn, F. Zhang, K. Wei, D. A. Rao, C. Rozo, U. K. Sokhi, S. Shanaj, D. J. Oliver, A. P. Echeverria, E. F. DiCarlo, M. B. Brenner, V. P. Bykerk, S. M. Goodman, S. Raychaudhuri, G. Rätsch, L. B. Ivashkiv, L. T. Donlin, HBEGF^{+} macrophages in rheumatoid arthritis induce fibroblast invasiveness. *Sci. Transl. Med.* **11**, eaau8587 (2019).
14. D. A. Rao, M. F. Gurish, J. L. Marshall, K. Slowikowski, C. Y. Fonseka, Y. Liu, L. T. Donlin, L. A. Henderson, K. Wei, F. Mizoguchi, N. C. Teslovich, M. E. Weinblatt, E. M. Massarotti, J. S. Coblyn, S. M. Helfgott, Y. C. Lee, D. J. Todd, V. P. Bykerk, S. M. Goodman, A. B. Pernis, L. B. Ivashkiv, E. W. Karlson, P. A. Nigrovic, A. Filer, C. D. Buckley, J. A. Lederer, S. Raychaudhuri, M. B. Brenner, Pathologically expanded peripheral T helper cell subset drives B cells in rheumatoid arthritis. *Nature* **542**, 110–114 (2017).
15. F. Zhang, K. Wei, K. Slowikowski, C. Y. Fonseka, D. A. Rao, S. Kelly, S. M. Goodman, D. Tabechian, L. B. Hughes, K. Salomon-Escoto, G. F. M. Watts, A. H. Jonsson, J. Rangel-Moreno, N. Meednu, C. Rozo, W. Apruzzese, T. M. Eisenhaure, D. J. Lieb, D. L. Boyle, A. M. Mandelin II; Accelerating Medicines Partnership Rheumatoid Arthritis, Systemic Lupus Erythematosus (AMP RA/SLE) Consortium, B. F. Boyce, E. D. Carlo, E. M. Gravallese, P. K. Gregersen, L. Moreland, G. S. Firestein, N. Hacohen, C. Nusbaum, J. A. Lederer, H. Perlman, C. Pitzalis, A. Filer, V. M. Holers, V. P. Bykerk, L. T. Donlin, J. H. Anolik, M. B. Brenner, S. Raychaudhuri, Defining inflammatory cell states in rheumatoid arthritis joint synovial tissues by integrating single-cell transcriptomics and mass cytometry. *Nat. Immunol.* **20**, 928–942 (2019).
16. J. J. Haringman, D. M. Gerlag, A. H. Zwinderman, T. J. M. Smeets, M. C. Kraan, D. Baeten, I. B. McInnes, B. Bresnihan, P. P. Tak, Synovial tissue macrophages: A sensitive biomarker for response to treatment in patients with rheumatoid arthritis. *Ann. Rheum. Dis.* **64**, 834–838 (2005).
17. A. M. Mandelin, P. J. Homan, A. M. Shaffer, C. M. Cuda, S. T. Dominguez, E. Bacalao, M. Carns, M. Hinchcliff, J. Lee, K. Aren, A. Thakrar, A. B. Montgomery, S. L. Bridges, J. M. Bathon, J. P. Atkinson, D. A. Fox, E. L. Matteson, C. D. Buckley, C. Pitzalis, D. Parks, L. B. Hughes, L. Geraldino-Pardilla, R. Ike, K. Phillips, K. Wright, A. Filer, S. Kelly, E. M. Ruderman, V. Morgan, H. Abdala-Valencia, A. V. Misharin, G. S. Budinger, E. T. Bartom, R. M. Pope, H. Perlman, D. R. Winter, S. L. Bridges, J. M. Bathon, J. P. Atkinson, D. A. Fox, E. L. Matteson, C. D. Buckley, C. Pitzalis, D. Parks, L. B. Hughes, L. Geraldino-Pardilla, R. Ike, K. Phillips, K. Wright, A. Filer, S. Kelly, E. M. Ruderman, V. Morgan, H. Abdala-Valencia, A. V. Misharin, G. S. Budinger, E. T. Bartom, R. M. Pope, H. Perlman, D. R. Winter, Transcriptional profiling of synovial macrophages using minimally invasive ultrasound-guided synovial biopsies in rheumatoid arthritis. *Arthritis Rheumatol.* **70**, 841–854 (2018).
18. S. Alivernini, L. MacDonald, A. Elmesmari, S. Finlay, B. Tolusso, M. R. Gigante, L. Petricca, C. di Mario, L. Bui, S. Perniola, M. Attar, M. Gessi, A. L. Fedele, S. Chilaka, D. Somma, S. N. Sansom, A. Filer, C. McSharry, N. L. Millar, K. Kirschner, A. Nerviani, M. J. Lewis, C. Pitzalis, A. R. Clark, G. Ferraccioli, I. Udalova, C. D. Buckley, E. Gremese, I. B. McInnes, T. D. Otto, M. Kurowska-Stolarska, Distinct synovial tissue macrophage subsets regulate inflammation and remission in rheumatoid arthritis. *Nat. Med.* **26**, 1295–1306 (2020).
19. B. M. Coates, K. L. Staricha, C. M. Koch, Y. Cheng, D. K. Shumaker, G. R. S. Budinger, H. Perlman, A. V. Misharin, K. M. Ridge, Inflammatory monocytes drive influenza A virus-mediated lung injury in juvenile mice. *J. Immunol.* **200**, 2391–2404 (2018).
20. M. Liao, Y. Liu, J. Yuan, Y. Wen, G. Xu, J. Zhao, L. Cheng, J. Li, X. Wang, F. Wang, L. Liu, I. Amit, S. Zhang, Z. Zhang, Single-cell landscape of bronchoalveolar immune cells in patients with COVID-19. *Nat. Med.* **26**, 842–844 (2020).
21. M. Merad, J. C. Martin, Pathological inflammation in patients with COVID-19: A key role for monocytes and macrophages. *Nat. Rev. Immunol.* **20**, 355–362 (2020).
22. J. F.-W. Chan, S. Yuan, K.-H. Kok, K. K.-W. To, H. Chu, J. Yang, F. Xing, J. Liu, C. C.-Y. Yip, R. W.-S. Poon, H.-W. Tsoi, S. K.-F. Lo, K.-H. Chan, V. K.-M. Poon, W.-M. Chan, J. D. Ip, J.-P. Cai, V. C.-C. Cheng, H. Chen, C. K.-M. Hui, K.-Y. Yuen, A familial cluster of pneumonia associated with the 2019 novel coronavirus indicating person-to-person transmission: A study of a family cluster. *Lancet* **395**, 514–523 (2020).
23. N. Zhu, D. Zhang, W. Wang, X. Li, B. Yang, J. Song, X. Zhao, B. Huang, W. Shi, R. Lu, P. Niu, F. Zhan, X. Ma, D. Wang, W. Xu, G. Wu, G. F. Gao, W. Tan; China Novel Coronavirus Investigating and Research Team, A novel coronavirus from patients with pneumonia in China, 2019. *N. Engl. J. Med.* **382**, 727–733 (2020).
24. J. Xue, S. V. V. Schmidt, J. Sander, A. Draffehn, W. Krebs, I. Quester, D. de Nardo, T. D. D. Gohel, M. Emde, L. Schmidleithner, H. Ganesan, A. Nino-Castro, M. R. R. Mallmann, L. Labzin, H. Theis, M. Kraut, M. Beyer, E. Latz, T. C. C. Freeman, T. Ulas, J. L. L. Schultze, D. de Nardo, T. D. D. Gohel, M. Emde, L. Schmidleithner, H. Ganesan, A. Nino-Castro, M. R. R. Mallmann, L. Labzin, H. Theis, M. Kraut, M. Beyer, E. Latz, T. C. C. Freeman, T. Ulas, J. L. L. Schultze, Transcriptome-based network analysis reveals a spectrum model of human macrophage activation. *Immunity* **40**, 274–288 (2014).
25. E. Y. Kim, H. Ner-Gaon, J. Varon, A. M. Cullen, J. Guo, J. Choi, D. Barragan-Bradford, A. Higuera, M. Pinilla-Vera, S. A. Short, A. Arciniegas-Rubio, T. Tamura, D. E. Leaf, R. M. Baron, T. Shay, M. B. Brenner, Post-sepsis immunosuppression depends on NKT cell regulation of mTOR/IFN-γ in NK cells. *J. Clin. Invest.* **130**, 3238–3252 (2020).
26. S. Ehrt, D. Schnappinger, S. Bekiranov, J. Drenkow, S. Shi, T. R. Gingeras, T. Gaasterland, G. Schoolnik, C. Nathan, Reprogramming of the macrophage transcriptome in response to interferon-gamma and Mycobacterium tuberculosis: Signaling roles of nitric oxide synthase-2 and phagocyte oxidase. *J. Exp. Med.* **194**, 1123–1140 (2001).
27. D. M. Mosser, J. P. Edwards, Exploring the full spectrum of macrophage activation. *Nat. Rev. Immunol.* **8**, 958–969 (2008).
28. T. K. Held, X. Weihua, L. Yuan, D. V. Kalvakolanu, A. S. Cross, Gamma interferon augments macrophage activation by lipopolysaccharide by two distinct mechanisms, at the signal transduction level and via an autocrine mechanism involving tumor necrosis factor alpha and interleukin-1. *Infect. Immun.* **67**, 206–212 (1999).
29. C. Wu, Y. Xue, P. Wang, L. Lin, Q. Liu, N. Li, J. Xu, X. Cao, IFN-γ primes macrophage activation by increasing phosphatase and tensin homolog via downregulation of miR-3473b. *J. Immunol.* **193**, 3036–3044 (2014).
30. X. Su, Y. Yu, Y. Zhong, E. G. Giannopoulou, X. Hu, H. Liu, J. R. Cross, G. Rätsch, C. M. Rice, L. B. Ivashkiv, Interferon-γ regulates cellular metabolism and mRNA translation to potentiate macrophage activation. *Nat. Immunol.* **16**, 838–849 (2015).
31. E. Latz, T. S. Xiao, A. Stutz, Activation and regulation of the inflammasomes. *Nat. Rev. Immunol.* **13**, 397–411 (2013).
32. A. Bouchon, M. Cella, H. L. Grierson, J. I. Cohen, M. Colonna, Activation of NK cell-mediated cytotoxicity by a SAP-independent receptor of the CD2 family. *J. Immunol.* **167**, 5517–5521 (2001).
33. P. R. Kumaresan, W. C. Lai, S. S. Chuang, M. Bennett, P. A. Mathew, CS1, a novel member of the CD2 family, is homophilic and regulates NK cell function. *Mol. Immunol.* **39**, 1–8 (2002).
34. J. J. Murphy, P. Hobby, J. Vilarino-Varela, B. Bishop, P. Iordanidou, B. J. Sutton, J. D. Norton, A novel immunoglobulin superfamily receptor (19A) related to CD2 is expressed on activated lymphocytes and promotes homotypic B-cell adhesion. *Biochem. J.* **361**, 431–436 (2002).
35. M. P. Karampetsou, D. Comte, K. Kis-Toth, V. C. Kyttaris, G. C. Tsokos, Expression patterns of signaling lymphocytic activation molecule family members in peripheral blood mononuclear cell subsets in patients with systemic lupus erythematosus. *PLOS ONE* **12**, e0186073 (2017).

36. J. de Salort, J. Sintes, L. Llinàs, J. Matesanz-Isabel, P. Engel, Expression of SLAM (CD150) cell-surface receptors on human B-cell subsets: From pro-B to plasma cells. *Immunol. Lett.* **134**, 129–136 (2011).
37. A. Veillette, SLAM-family receptors: Immune regulators with or without SAP-family adaptors. *Cold Spring Harb. Perspect. Biol.* **2**, a002469 (2010).
38. Z. Xia, M. Gu, X. Jia, X. Wang, C. Wu, J. Guo, L. Zhang, Y. Du, J. Wang, Integrated DNA methylation and gene expression analysis identifies SLAMF7 as a key regulator of atherosclerosis. *Aging* **10**, 1324–1337 (2018).
39. T. Maekawa, S. Kato, T. Kawamura, K. Takada, T. Sone, H. Ogata, K. Saito, T. Izumi, S. Nagao, K. Takano, Y. Okada, N. Tachi, M. Teramoto, T. Horiuchi, R. Hikota-Saga, K. Endo-Umeda, S. Uno, Y. Osawa, A. Kobayashi, S. Kobayashi, K. Sato, M. Hashimoto, S. Suzu, K. Usuki, S. Morishita, M. Araki, M. Makishima, N. Komatsu, F. Kimura, Increased SLAMF7 ^{high} monocytes in myelofibrosis patients harboring *JAK2* V617F provide a therapeutic target of elotuzumab. *Blood* **134**, 814–825 (2019).
40. J. R. Kim, S. O. Mathew, P. A. Mathew, Blimp-1/PRDM1 regulates the transcription of human CS1 (SLAMF7) gene in NK and B cells. *Immunobiology* **221**, 31–39 (2016).
41. A. Viola, F. Munari, R. Sánchez-Rodríguez, T. Scolaro, A. Castegna, The metabolic signature of macrophage responses. *Front. Immunol.* **10**, 1462 (2019).
42. M. Trizzino, A. Zucco, S. Deliard, F. Wang, E. Barbieri, F. Veglia, D. Gabrilovich, A. Gardini, EGR1 is a gatekeeper of inflammatory enhancers in human macrophages. *Sci. Adv.* **7**, eaaz8836 (2021).
43. M. Y. Bhat, H. S. Solanki, J. Advani, A. A. Khan, T. S. Keshava Prasad, H. Gowda, S. Thiyagarajan, A. Chatterjee, Comprehensive network map of interferon gamma signaling. *J. Cell Commun. Signal.* **12**, 745–751 (2018).
44. G. L. Plosker, Ruxolitinib: A review of its use in patients with myelofibrosis. *Drugs* **75**, 297–308 (2015).
45. L. Hui, L. Qi, H. Guoyu, S. Xuliang, T. Meiao, Ruxolitinib for treatment of steroid-refractory graft-versus-host disease in adults: A systematic review and meta-analysis. *Expert Rev. Hematol.* **13**, 565–575 (2020).
46. J. R. Kim, N. C. Horton, S. O. Mathew, P. A. Mathew, CS1 (SLAMF7) inhibits production of proinflammatory cytokines by activated monocytes. *Inflamm. Res.* **62**, 765–772 (2013).
47. P. O'Connell, Y. Pepelyayeva, M. K. Blake, S. Hyslop, R. B. Crawford, M. D. Rizzo, C. Pereira-Hicks, S. Godbehere, L. Dale, P. Gulick, N. E. Kaminski, A. Amalfitano, Y. A. Aldhamen, P. O'Connell, Y. Pepelyayeva, M. K. Blake, S. Hyslop, R. B. Crawford, M. D. Rizzo, C. Pereira-Hicks, S. Godbehere, L. Dale, P. Gulick, N. E. Kaminski, A. Amalfitano, Y. A. Aldhamen, SLAMF7 is a critical negative regulator of IFN-α-mediated CXCL10 production in chronic HIV infection. *J. Immunol.* **202**, 228–238 (2019).
48. J. Kikuchi, M. Hori, H. Iha, N. Toyama-Sorimachi, S. Hagiwara, Y. Kuroda, D. Koyama, T. Izumi, H. Yasui, A. Suzuki, Y. Furukawa, Soluble SLAMF7 promotes the growth of myeloma cells via homophilic interaction with surface SLAMF7. *Leukemia* **34**, 180–195 (2020).
49. A. Friedman, C/EBPalpha induces PU.1 and interacts with AP-1 and NF-kappaB to regulate myeloid development. *Blood Cells Mol. Dis.* **39**, 340–343 (2007).
50. J. Zhou, H. Li, X. Xia, A. Herrera, N. Pollock, V. Reebye, M. H. Sodergren, S. Dorman, B. H. Littman, D. Doogan, K.-W. Huang, R. Habib, D. Blakey, N. A. Habib, J. J. Rossi, Anti-inflammatory activity of MTL-CEBPA, a small activating RNA drug, in LPS-stimulated monocytes and humanized mice. *Mol. Ther.* **27**, 999–1016 (2019).
51. C. A. Donado, A. B. Cao, D. P. Simmons, B. A. Croker, P. J. Brennan, M. B. Brenner, A two-cell model for IL-1β release mediated by death-receptor signaling. *Cell Rep.* **31**, 107466 (2020).
52. F. O. Martinez, S. Gordon, M. Locati, A. Mantovani, Transcriptional profiling of the human monocyte-to-macrophage differentiation and polarization: New molecules and patterns of gene expression. *J. Immunol.* **177**, 7303–7311 (2006).
53. K. Kang, M. Bachu, S. H. Park, K. Kang, S. Bae, K.-H. Park-Min, L. B. Ivashkiv, IFN-γ selectively suppresses a subset of TLR4-activated genes and enhancers to potentiate macrophage activation. *Nat. Commun.* **10**, 3320 (2019).
54. N. Wu, A. Veillette, SLAM family receptors in normal immunity and immune pathologies. *Curr. Opin. Immunol.* **38**, 45–51 (2016).
55. B. J. van Driel, G. Liao, P. Engel, C. Terhorst, Responses to microbial challenges by SLAMF receptors. *Front. Immunol.* **7**, 4 (2016).
56. I. Tassi, M. Colonna, The cytotoxicity receptor CRACC (CS-1) recruits EAT-2 and activates the PI3K and phospholipase Cgamma signaling pathways in human NK cells. *J. Immunol.* **175**, 7996–8002 (2005).
57. J. Chen, M.-C. Zhong, H. Guo, D. Davidson, S. Mishel, Y. Lu, I. Rhee, L.-A. Pérez-Quintero, S. Zhang, M.-E. Cruz-Munoz, N. Wu, D. C. Vinh, M. Sinha, V. Calderon, C. A. Lowell, J. S. Danska, A. Veillette, SLAMF7 is critical for phagocytosis of haematopoietic tumour cells via Mac-1 integrin. *Nature* **544**, 493–497 (2017).
58. T. Joshi, J. P. Butchar, S. Tridandapani, Fcgamma receptor signaling in phagocytes. *Int. J. Hematol.* **84**, 210–216 (2006).
59. S. Fodor, Z. Jakus, A. Mócsai, ITAM-based signaling beyond the adaptive immune response. *Immunol. Lett.* **104**, 29–37 (2006).
60. A. Mócsai, J. Ruland, V. L. J. Tybulewicz, The SYK tyrosine kinase: A crucial player in diverse biological functions. *Nat. Rev. Immunol.* **10**, 387–402 (2010).
61. Y.-S. Yi, Y.-J. Son, C. Ryou, G. H. Sung, J. H. Kim, J. Y. Cho, Functional roles of Syk in macrophage-mediated inflammatory responses. *Mediators inflamm.* **2014**, 270302 (2014).
62. J. M. Gane, R. A. Stockley, E. Sapey, TNF-α autocrine feedback loops in human monocytes: The pro- and anti-inflammatory roles of the TNF-α receptors support the concept of selective TNFR1 blockade in vivo. *J. Immunol. Res.* **2016**, 1079851 (2016).
63. L. M. Donald, S. Alivernini, B. Tolusso, A. Elmesmari, D. Somma, S. Perniola, A. Paglionico, L. Petricca, S. L. Bosello, A. Carfì, M. Sali, E. Stigliano, A. Cingolani, R. Murri, V. Arena, M. Fantoni, M. Antonelli, F. Landi, F. Franceschi, M. Sanguinetti, I. B. M. Innes, C. M. Sharry, A. Gasbarrini, T. D. Otto, M. Kurowska-Stolarska, E. Gremese, COVID-19 and RA share an SPP1 myeloid pathway that drives PD-L1+ neutrophils and CD14+ monocytes. *JCI Insight* **6**, e147413 (2021).
64. F. Zhang, J. R. Mears, L. Shakib, J. I. Beynor, S. Shanaj, I. Korsunsky, A. Nathan; Accelerating Medicines Partnership Rheumatoid Arthritis, Systemic Lupus Erythematosus (AMP RA/SLE) Consortium, L. T. Donlin, S. Raychaudhuri, IFN-γ and TNF-α drive a *CXCL10+ CCL2+* macrophage phenotype expanded in severe COVID-19 lungs and inflammatory diseases with tissue inflammation. *Genome Med.* **13**, 64 (2021).
65. J. D. Malaer, P. A. Mathew, CS1 (SLAMF7, CD319) is an effective immunotherapeutic target for multiple myeloma. *Am. J. Cancer Res.* **7**, 1637–1641 (2017).
66. T. Pazina, A. M. James, A. W. MacFarlane, N. A. Bezman, K. A. Henning, C. Bee, R. F. Graziano, M. D. Robbins, A. D. Cohen, K. S. Campbell, The anti-SLAMF7 antibody elotuzumab mediates NK cell activation through both CD16-dependent and -independent mechanisms. *Onco. Targets. Ther.* **6**, e1339853 (2017).
67. A. T. Kurdi, S. V. Glavey, N. A. Bezman, A. Jhatakia, J. L. Guerriero, S. Manier, M. Moschetta, Y. Mishima, A. Roccaro, A. Detappe, C.-J. Liu, A. Sacco, D. Huynh, Y.-T. Tai, M. D. Robbins, J. Azzi, I. M. Ghobrial, Antibody-dependent cellular phagocytosis by macrophages is a novel mechanism of action of elotuzumab. *Mol. Cancer Ther.* **17**, 1454–1463 (2018).
68. J. Woo, M. P. Vierboom, H. Kwon, D. Chao, S. Ye, J. Li, K. Lin, I. Tang, N. A. Belmar, T. Hartman, E. Breedveld, V. Vexler, B. A. 't Hart, D. A. Law, G. C. Starling, PDL241, a novel humanized monoclonal antibody, reveals CD319 as a therapeutic target for rheumatoid arthritis. *Arthritis Res. Ther.* **15**, R207 (2013).
69. D. Aletaha, T. Neogi, A. J. Silman, J. Funovits, D. T. Felson, C. O. Bingham, N. S. Birnbaum, G. R. Burmester, V. P. Bykerk, M. D. Cohen, B. Combe, K. H. Costenbader, M. Dougados, P. Emery, G. Ferraccioli, J. M. W. Hazes, K. Hobbs, T. W. J. Huizinga, A. Kavanaugh, J. Kay, T. K. Kvien, T. Laing, P. Mease, H. A. Ménard, L. W. Moreland, R. L. Naden, T. Pincus, J. S. Smolen, E. Stanislawska-Biernat, D. Symmons, P. P. Tak, K. S. Upchurch, J. Vencovský, F. Wolfe, G. Hawker, 2010 Rheumatoid arthritis classification criteria: An American College of Rheumatology/European League Against Rheumatism collaborative initiative. *Arthritis Rheum.* **62**, 2569–2581 (2010).
70. L. T. Donlin, D. A. Rao, K. Wei, K. Slowikowski, M. J. McGeachy, J. D. Turner, N. Meednu, F. Mizoguchi, M. Gutierrez-Arcelus, D. J. Lieb, J. Keegan, K. Muskat, J. Hillman, C. Rozo, E. Ricker, T. M. Eisenhaure, S. Li, E. P. Browne, A. Chicoine, D. Sutherby, A. Noma, C. Nusbaum, S. Kelly, A. B. Pernis, L. B. Ivashkiv, S. M. Goodman, W. H. Robinson, P. J. Utz, J. A. Lederer, E. M. Gravallese, B. F. Boyce, N. Hacohen, C. Pitzalis, P. K. Gregersen, G. S. Firestein, S. Raychaudhuri, L. W. Moreland, V. M. Holers, V. P. Bykerk, A. Filer, D. L. Boyle, M. B. Brenner, J. H. Anolik, Methods for high-dimensional analysis of cells dissociated from cryopreserved synovial tissue. *Arthritis Res. Ther.* **20**, 139 (2018).
71. S. Picelli, Å. K. Björklund, O. R. Faridani, S. Sagasser, G. Winberg, R. Sandberg, Smart-seq2 for sensitive full-length transcriptome profiling in single cells. *Nat. Methods* **10**, 1096–1098 (2013).
72. S. Picelli, O. R. Faridani, A. K. Björklund, G. Winberg, S. Sagasser, R. Sandberg, Full-length RNA-seq from single cells using Smart-seq2. *Nat. Protoc.* **9**, 171–181 (2014).
73. J. J. Trombetta, D. Gennert, D. Lu, R. Satija, A. K. Shalek, A. Regev, Preparation of single-cell RNA-seq libraries for next generation sequencing. *Curr. Protoc. Mol. Biol.* **107**, 4.22.1–4.22.17 (2014).
74. A. Dobin, C. A. Davis, F. Schlesinger, J. Drenkow, C. Zaleski, S. Jha, P. Batut, M. Chaisson, T. R. Gingeras, STAR: Ultrafast universal RNA-seq aligner. *Bioinformatics* **29**, 15–21 (2013).
75. B. Li, C. N. Dewey, RSEM: Accurate transcript quantification from RNA-Seq data with or without a reference genome. *BMC Bioinformatics.* **12**, 323 (2011).
76. A. Zhu, J. G. Ibrahim, M. I. Love, Heavy-tailed prior distributions for sequence count data: Removing the noise and preserving large differences. *Bioinformatics* **35**, 2084–2092 (2019).
77. N. L. Bray, H. Pimentel, P. Melsted, L. Pachter, Near-optimal probabilistic RNA-seq quantification. *Nat. Biotechnol.* **34**, 525–527 (2016).
78. M. I. Love, W. Huber, S. Anders, Moderated estimation of fold change and dispersion for RNA-seq data with DESeq2. *Genome Biol.* **15**, 550 (2014).
79. G. Korotkevich, V. Sukhov, N. Budin, B. Shpak, M. N. Artyomov, A. Sergushichev, Fast gene set enrichment analysis. *bioRxiv* , 060012 (2019).
80. A. Butler, P. Hoffman, P. Smibert, E. Papalexi, R. Satija, Integrating single-cell transcriptomic data across different conditions, technologies, and species. *Nat. Biotechnol.* **36**, 411–420 (2018).

81. T. Stuart, A. Butler, P. Hoffman, C. Hafemeister, E. Papalexi, W. M. Mauck, Y. Hao, M. Stoeckius, P. Smibert, R. Satija, Comprehensive integration of single-cell data. *Cell* **177**, 1888–1902.e21 (2019).
82. I. Korsunsky, N. Millard, J. Fan, K. Slowikowski, F. Zhang, K. Wei, Y. Baglaenko, M. Brenner, P.-R. Loh, S. Raychaudhuri, Fast, sensitive and accurate integration of single-cell data with Harmony. *Nat. Methods* **16**, 1289–1296 (2019).

Acknowledgments: We thank F. Zhang, I. Korsunsky, and S. Raychaudhuri for the advice on bioinformatic analysis; M. Gurish and G. Keras for the assistance recruiting patients and processing samples; W. Apruzzese for the helpful discussions; J. Toska for the help with Western blots; and patients for the participation. Sorting was performed in the BWH Human Immunology Center. We thank the members of the AMP RA/SLE Phase 1 Network for their contributions. **Funding:** This work was supported by NIH NIAID P01AI148102, NIH NIAMS P30 AR070253, and the Accelerating Medicines Partnership (AMP) in Rheumatoid Arthritis and Lupus Network. AMP is a public-private partnership (AbbVie Inc.; Arthritis Foundation; Bristol-Myers Squibb Company; Foundation for the NIH; GlaxoSmithKline; Janssen Research and Development, LLC; Lupus Foundation of America; Lupus Research Alliance; Merck Sharp & Dohme Corp.; National Institute of Allergy and Infectious Diseases; National Institute of Arthritis and Musculoskeletal and Skin Diseases; Pfizer Inc.; Rheumatology Research Foundation; and Sanofi and Takeda Pharmaceuticals International Inc.) created to develop new ways of identifying and validating promising biological targets for diagnostics and drug development. Funding for AMP was provided through grants from the NIH (UH2-AR067676, UH2-AR067677, UH2-AR067679, UH2-AR067681, UH2-AR067685, UH2- AR067688, UH2-AR067689, UH2-AR067690, UH2-AR067691, UH2-AR067694, and UM2- AR067678). D.P.S. was supported by Institutional Training Grant NIH NHLBI T32 HL007627 and NIH NIAMS K08 AR075850. **Author contributions:** Conceptualization: D.P.S., D.A.R., and M.B.B. Methodology: D.P.S., H.N.N., and E.G.-R. Formal analysis: D.P.S., and Y.J. Investigation: D.P.S., H.N.N., and E.G.-R. Resources: D.P.S., E.G.-R., A.H.J., A.F.C., J.K.L., G.S.D., P.B., B.E.E., J.S.C., E.M.M., J.A.S., and D.J.T. Data curation: D.P.S. Writing—original draft: D.P.S. Writing—review and editing: D.P.S., H.N.N., E.G.-R., Y.J., A.H.J., A.F.C., J.K.L., G.S.D., P.B., B.E.E., J.S.C., E.M.M., J.A.S., D.J.T., D.A.R., E.Y.K., and M.B.B. Visualization: D.P.S. Supervision: M.B.B. Project administration: D.A.R. and M.B.B. Funding acquisition: D.P.S. and M.B.B. **Competing interests:** The authors declare that they have no competing interests. Accelerating Medicines Partnership and AMP are registered service marks of the U.S. Department of Health and Human Services. **Data and materials availability:** RNA-seq of sorted monocyte populations with high and low expression of SLAMF7 are available at NCBI GEO GSE185508. RNA-seq from in vitro–stimulated monocyte-derived macrophages is available at NCBI GEO GSE185509. All other data needed to evaluate the conclusions in the paper are present in the paper or the Supplementary Materials.

Individual members of the AMP RA/SLE Phase 1 Network are listed alphabetically:
Jen Anolik, William Apruzzese, Joan M. Bathon, Ami Ben-Artzi, David L. Boyle, Brendan Boyce, S. Louis Bridges, Vivian Bykerk, Kevin Deane, Edward DiCarlo, Laura Donlin, Tom Eisenhaure, Andrew Filer, Gary S. Firestein, Lindsy Forbess, Susan Goodman, Ellen Gravallese, Peter K. Gregersen, Joel Guthridge, V. Michael Holers, Diane Horowitz, Laura Hughes, Judith James, James Lederer, Arthur Mandelin, Mandy McGeachy, Larry Moreland, Nir Hacohen, Harris Perlman, Costantino Pitzalis, Soumya Raychaudhuri, Christopher Ritchlin, Bill Robinson, Jennifer Seifert, P. J. Utz, Kevin Wei, Fan Zhang.

Submitted 15 October 2020
Resubmitted 1 October 2021
Accepted 20 January 2022
Published 11 February 2022
10.1126/sciimmunol.abf2846

Science Immunology

SLAMF7 engagement superactivates macrophages in acute and chronic inflammation

Daimon P. SimmonsHung N. NguyenEmma Gomez-RivasYunju JeongA. Helena JonssonAntonia F. ChenJeffrey K. LangeGeorge S. DyerPhilip BlazarBrandon E. EarpJonathan S. CoblynElena M. MassarottiJeffrey A. SparksDerrick J. ToddDeepak A. RaoEdy Y. KimMichael B. Brenner

Sci. Immunol., 7 (68), eabf2846. • DOI: 10.1126/sciimmunol.abf2846

Inflammatory macrophages get supercharged

Macrophages produce inflammatory cytokines that stimulate immune responses against pathogens, but excessive or chronic activation in inflammatory diseases can lead to tissue damage. By profiling synovial macrophages, Simmons *et al.* found that SLAM family member (SLAMF7) was elevated in patients with rheumatoid arthritis (RA) compared with less inflammatory osteoarthritis and could be induced by IFN-#. Signaling through SLAMF7 in macrophages stimulated a cascade of inflammatory cytokine production that was further amplified by autocrine TNF. Macrophages from patients with inflammatory bowel disease or COVID-19 also expressed a transcriptional profile of dysfunctional SLAMF7-driven activation that was correlated with disease activity, demonstrating that SLAMF7-associated macrophage activation occurs during both acute and chronic human inflammatory diseases.

Science Immunology (ISSN) is published by the American Association for the Advancement of Science. 1200 New York Avenue NW, Washington, DC 20005. The title *Science Immunology* is a registered trademark of AAAS.